Analysing the impact of trap shape and movement behaviour of ground-dwelling arthropods on trap efficiency

D.A. Ahmed*[1] and S.V. Petrovskii†[2,3]

[1]Center for Applied Mathematics and Bioinformatics (CAMB), Department of Mathematics and Natural Sciences, Gulf University for Science and Technology, P.O. Box 7207, Hawally 32093, Kuwait

[2]Department of Mathematics, University of Leicester, University road, Leicester, LE1 7RH, UK

[3]Peoples Friendship University of Russia (RUDN University), 6 Miklukho-Maklaya St, Moscow 117198, Russian Federation

Keywords:

Pitfall traps, Trap efficiency, Insect modelling, Pest monitoring, Random walks, Brownian motion, Correlated random walk, Lévy walks.

Abstract

1. The most reliable estimates of the population abundance of ground-dwelling arthropods are obtained almost entirely through trap counts. Trap shape can be easily controlled by the researcher, commonly the same trap design is employed in all sites within a given study. Few researchers really try to compare abundances (numbers of collected individuals) between studies because these are heavily influenced by environmental conditions, e.g. temperature, habitat structure, food sources available, directly affecting insect movement activity.

2. We propose that useful insights can be obtained from a theoretical based approach. We focus on the interplay between trap shape (circle, square, slot), the underlying movement behaviour and the subsequent effect on captures. We simulate trap counts within these different geometries whilst considering movement processes with clear distinct properties, such as Brownian motion (BM), the Correlated Random Walk (CRW) and the Lévy walk (LW).

3. (i) We find that slot shaped traps are far less efficient than circular or square traps assuming same perimeter length, with differences which can exceed more than two-fold. Such impacts

*Ahmed.D@gust.edu.kw

†sp237@le.ac.uk

of trap geometry are only realised if insect mobility is sufficiently large, which is known to significantly vary depending on type of habitat.

(ii) If the movement pattern incorporates localized forward persistence then trap counts accumulate at a much slower rate, and this rate decreases further with higher persistency.

(iii) If the movement behaviour is of Lévy type, then fastest catch rates are recorded in the case of circular trap, and the slowest for the slot trap, indicating that trap counts can strongly depend on trap shape. Lévy walks exacerbate the impact of geometry while correlated random walks make these differences more inconsequential.

4. In this study we reveal trap efficiencies and how movement type can alter capture rates. Such information contributes towards improved trap count interpretations, as required in ecological studies which make use of trapping systems.

1 Introduction

Trapping of insects is central to many ecological studies, particularly in ecosystem services ecology (Work et al., 2002). For ground-dwelling (surface-active) arthropods, pitfall traps are most frequently used to collect trap count samples, which are then manipulated to obtain information on structure of communities (Hammond, 1990), habitat associations (Honêk, 1988), activity patterns (Den Boer, 1981), spatial distribution (Niemelä et al., 1990), relative abundances (Desender and Maelfait, 1986), total population estimates (Mommertz et al., 1996) and distribution ranges (Giblin-Davis et al., 1994). Most common sampled species include; ground beetles (*Coleoptera: Carabidae*), rove beetles (*Coleoptera: Staphylinidae*), wandering spiders (*Aranae: Lycosidae* and *Clubionidae*), and ants (*Hymenoptera: Formicidae*) (Woodcock, 2005). The advantages of such a sampling technique is that pitfall traps are simple to install, easy to transport and cost-effective, studies are easy to replicate and enable large data collection useful for statistical analyses (Greenslade, 1964). Pitfall traps are also used for general survey of insect diversity, detection of new invasions of insect pests for delimitation of area of infestation, and for monitoring population levels of established pests. Such information aids the decision making process for the initiation of control measures or to measure effectiveness of a pest management program (Pimentel, 2009). Mass trapping is an example of a direct control strategy, that aims to reduce the rate of increase in a population by removing a large number of insects (El-Sayed et al., 2006). Another example which is different from pitfall trapping, but equally as relevant, and suggested to have great potential is the installation of trap crops, which are plant stands that are grown to attract pests to reduce pest density in the main crop (Hannunen, 2005).

Despite frequent use, the issue is that trap captures can be influenced by variation in trap design, such as shape, size, quantity, spatial arrangement, material, type of preservative used (Luff, 1975; Pekár, 2002;

Koivula et al., 2003). Often, this leads to interpretation issues, e.g. if trap size is unnecessarily large, sample counts can be distorted due to unwanted by-catches of non-target insects or even non-arthropods (Pearce et al., 2005). These factors can be adjusted and modifications can be made in line with experimental requirements. In contrast, physical or biological factors amongst species which influence counts are much more difficult to control, such as inter/intra-individual individual differences (e.g. body mass, movement capabilities), ecological interactions, or those specific to the environment or habitat (e.g. temperature, rainfall, vegetation structure) (Melbourne, 1999; Saska et al., 2013). For some time now, ecologists have highlighted that since conclusions are drawn from samples and in turn used to make hypotheses about populations, the impact of these factors must be well understood (Cheli and Corley, 2010).

To increase trapping efficiency, many studies have attempted to propose improved trap designs, but much focus is on more practical details i.e. material construction (e.g. use of roof/funnels, plastic rims, guidance barriers) (Császár et al., 2018; Boetzl et al., 2018), albeit, few researchers have focused on other details, e.g. body mass, temperature (Koivula et al., 2003; Engel et al., 2017). We appreciate that such studies are informative, although very few address more fundamental questions relating to trap geometry or insect movement behaviour. Another issue is that there exists extreme variation in experimental design, and how counts are reported and interpreted (Brown and Matthews, 2016). Currently, the trend has been usage of an assortment of traps of different shapes and sizes at randomized spatial locations (Engel et al., 2017). The consequence is that the ability to draw meaningful comparisons across studies is severely hampered. Note that, in principle, standardization of pitfall traps does not necessarily translate to effective comparability in all cases, due to the sensitive nature of trap counts, as mentioned earlier, however, sound methodological reporting alongside a unified approach could potentially improve comparability. Better understanding of trap geometry and movement impacts would certainly contribute towards this process. Taking the above into account, it is not surprising that very few studies provide information on such impacts. Actually, we question whether such intricate information can really be obtained from field experiments, if catch rates are heavily influenced?

In this study, our focus is on trap shape and the subsequent impact, whilst considering different modes of movement. As a first step, it makes sense to work at the smallest spatial scale, that is in the case of a single trap. The trap shapes considered are those which are used in pitfall trapping studies, with the circular trap being most frequently used by consensus, and those used on occasion such as square and slot (rectangular trap shape, also called gutter) (Southwood, 1978; Blackshaw et al., 2018). We propose that a more effective and robust approach to investigate this issue is from a theoretical standpoint through simulations, whilst other empirical studies have led to inconsistent results (Spence and Niemelä, 1994). Simulations are cost effective, easy to replicate, and alternative information can be sought that normally would be difficult to obtain otherwise (Petrovskii and Petrovskaya, 2012). Most importantly, some of those

factors which are deemed difficult to control in a real-field, would now either be absent or controllable. For example, each individual can now be considered completely 'identical' with respect to physical and biological traits - whereas in the field, ground-dwelling arthropods have different body mass, can vary in stage of development (metamorphosis) or exhibit different movement capabilities even in the case of the same species (Petrovskii and Morozov, 2009; Engel et al., 2017). Any additional complexity due to environmental heterogeneity is also removed from the system e.g. effects of temperature or wind are absent.

The earliest modelling attempts for insect movement have been entirely based on Brownian motion (BM) and diffusion as the mean field counterpart - which have proven to be successful, especially at large time scales (Levin et al., 1984). This is partly due to the presumption that such species can be thought of as non-cognitive and thus completely random (Okubo, 1980). Examples of ecological applications include, conservation (Reichenbach et al., 2007), biological invasions (Hengeveld, 1989) and insect pest monitoring (Petrovskii et al., 2012, 2014), with attempts made for a variety of taxa, e.g. black veined white butterflies (*Aporia crataegi*) (Watanabe, 1978), slug parasitic nematode (*Phasmarhabditis hermaphrodita*) (Hapca et al., 2009) and walking beetles (*Tenebrio molitor*) (Bearup et al., 2016). Despite the success, it has been realised for some time now, that BM provides an oversimplified description on smaller time scales, not only for animals that exhibit cognitive abilities (e.g. mammals or reptiles) (Holmes, 1993) - which is expected, but also for ground-dwelling arthropods. As a result, models which are essentially non-Brownian have been developed, such as the Correlated Random Walk (CRW), which allows for forward directional persistence as opposed to being completely random (Kareiva and Shigesada, 1983). This provides a more accurate description of the movement trajectory, as individuals are more likely to maintain the same direction of travel or turn at small angles (Pyke, 2015). Some examples where the CRW model has been effective include; cabbage butterflies (*Pieris rapae*) (Kareiva and Shigesada, 1983), bark beetles (*Scolytinae*) (Byers, 2001), and *Leptothorax* ant colonies (Sendova and Lent, 2012).

The mechanisms behind individual insect movement can be more complicated than what BM and the CRW propose. In the literature, other more complicated processes have been documented, such as; intermittent stop-start movement (Mashanova et al., 2010), behavioural intensive-extensive changes (Knell and Codling, 2012), individual interactions (De Jager et al., 2012), density or time dependent diffusion (Ahmed and Petrovskii, 2015; Ellis et al., 2018), Lévy walks (Sims et al., 2008) or even a mixture or composition of the above (Auger-Méthé et al., 2015). The issue is more perplexing, since movement patterns can be misidentified (Petrovskii et al., 2011) or even, in the context of trapping, almost identical trap counts can be reproduced for inherently different movement models (Ahmed et al., 2018). Also, the conceptual case of BM is often revisited due to its relative simplicity and on occasion shown to be in excellent agreement with field data (Bearup et al., 2016). The commentary by Codling (2014) discusses

some of the current ongoing challenges in identifying the underlying movement model.

Provided the movement process and its properties are sufficiently known, we can simulate the movement track of each individual using a random walk framework, and by extension, the distribution of the population in space can be estimated (Grimm and Railsback, 2005). If we consider the motion of N individuals in a confined arena with trap installed, assuming no migration, mortality or reproduction and assume that the trap depth is deep enough so that no individual is prone to escape, then the total population can only decrease as a result of trapping. Trap counts are accumulated by removing those individuals from the system whose position lies within a predefined trapping region (Petrovskii et al., 2012). The resulting trap count trajectory is stochastic, and simulations can be averaged over multiple runs to reduce this effect - enabling comparability across different scenarios.

By consensus, the default trap shape is normally circular, however, there is no principal argument for this choice. The study by Spence and Niemelä (1994) demonstrated that circular pitfall traps yielded generally more catches than slot type, although they could not determine the rank of other types of pitfall traps, since captures were influenced by both species type and landscape. Another example is that by Baars (1979), who simulated single trap year-catches for ground beetles (*Pterostichus versicolor*), and found that circular traps were slightly more efficient than square type (see Table 10 in that paper). Elsewhere, simulation models have been used to optimize the spatial distribution and other features of traps in agricultural fields, especially trap cropping (Holden et al., 2012), but the geometry of these structures have very rarely been assessed on trapping efficiency, for e.g. Hannunen (2005) only consider slot shaped crop patches. We investigate this issue in more depth, with interest in the precise rank order of trap shapes in terms of efficiency and the corresponding trap count patterns that emerge. Identification of the optimal trap shape, and in general, better understanding of the interplay between trap shape and captures contributes towards the design of effective traps used to control pest insects or help improve surveys for detection of invasion species (Pimentel, 2009; Berec et al., 2015). This could also apply in the case of insect monitoring at multiple scales, where many traps are deployed over a large agricultural field or even on a landscape scale (Petrovskii et al., 2014). Such information would also be of particular interest to those who call for, and propose to develop a standard pitfall trap design (Brown and Matthews, 2016).

In this study, we consider movement models with clear distinct properties, namely, Brownian motion (BM), the Correlated Random Walk (CRW) and the Lévy walk (LW). Our aim is two-fold, firstly, to investigate the trapping efficiency of different trap shapes, and secondly, to reveal how capture rates are affected by these type of movement processes and to what extent. The focal point is to help better understand catch patterns in general - facilitating better trap count interpretations leading to practical applications.

2 Modelling framework

The movement path of an insect browsing in the field can be described by a continuous curved trajectory with position $\mathbf{r} = (x(t), y(t))$ at time t. For computational expediency, we discretize the movement path, so that each position $\mathbf{r}_i = \{\mathbf{r}_0, \mathbf{r}_1, \mathbf{r}_2, ..., \mathbf{r}_n, ...\}$ is recorded at discrete times $t_i = \{t_0, t_1, t_2, ..., t_n, ...\}$, with $i = 0, 1, 2, ..., n, ...$ steps (Turchin, 1998). If the initial position $\mathbf{r}_0 = (x_0, y_0)$ is prescribed at time $t = t_0 = 0$, then each subsequent position can be determined by the relation

$$\mathbf{r}_{i+1} = \mathbf{r}_i + (\Delta\mathbf{r})_i \quad \text{at time} \quad t_i = i\Delta t, \tag{2.0.1}$$

where movement data is assumed to be recorded at fixed time increments Δt. The step vector $(\Delta\mathbf{r})_i$ has components which can be written in either (a) cartesian co-ordinates $(\Delta\mathbf{r})_i = (\xi_i, \eta_i)$ where ξ, η are random variables for the horizontal/vertical components of each step, respectively, or in (b) polar co-ordinates $(\Delta\mathbf{r})_i = (l_i, \theta_i)$ with $l_i^2 = \xi_i^2 + \eta_i^2$, $\theta_i = \arctan_2(\eta_i, \xi_i)$, where $\arctan_2(\eta_i, \xi_i)$ is equal to $\arctan\left(\frac{\eta_i}{\xi_i}\right)$ for $\xi_i > 0$ and to $\arctan\left(\frac{\eta_i}{\xi_i}\right) \pm \pi$ radians for $\xi_i < 0$. The step vector is described in terms of the step length (also known as dispersal kernel) $l_i = |\mathbf{r}_{i+1} - \mathbf{r}_i| = \{l_0, l_1, ..., l_{n-1}\}$ and turning angle $\theta_i = \{\theta_0, \theta_1, ..., \theta_{n-1}\}$, measured clockwise from the line of direction at each heading. The characteristics of the movement process are determined by the statistical properties of the step length and turning angle probability distributions. Fig. 2.0.1 illustrates the random walk model in each co-ordinate system.

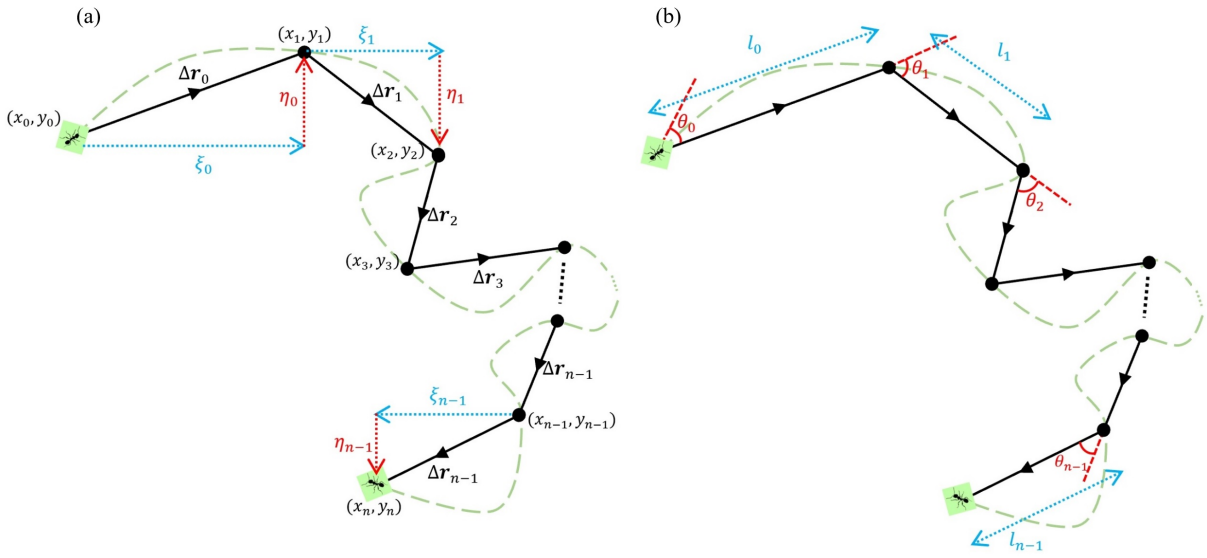

Figure 2.0.1: Random walk model: Insect begins at initial position $\mathbf{r}_0 = (x_0, y_0)$ at time $t = 0$. Subsequent positions are determined by (2.0.1), i.e. $\mathbf{r}_1 = \mathbf{r}_0 + (\Delta \mathbf{r})_0$, $\mathbf{r}_2 = \mathbf{r}_1 + (\Delta \mathbf{r})_1$, $\mathbf{r}_3 = \mathbf{r}_2 + (\Delta \mathbf{r})_2$ and so on, recorded at times $t = \Delta t, 2\Delta t, 3\Delta t, \ldots$ respectively. The step vector can be described either by (a) cartesian, $(\Delta \mathbf{r})_i = (\xi_i, \eta_i)$ i.e in terms of its horizontal/vertical components, or (b) polar: $(\Delta \mathbf{r})_i = (l_i, \theta_i)$ i.e in terms of step lengths and turning angles.

2.1 Brownian Motion (BM)

In case of BM the movement pattern is completely random and each component of the step vector (ξ_i, η_i) is normally distributed. Both step distributions have zero mean and the same variance σ^2, where σ is the mobility rate which determines insect activity. This implicitly assumes that the movement does not have any global directional bias and hence it occurs in an isotropic environment. In other words, there is no long-term drift which normally would arise due to external directional cues (taxis) or a response to an external stimulus (differential klino-kinesis) (Bailey et al., 2018). On a local level, we assume that there is no forward directional persistence and thus the movement process is essentially Markovian with regard to location. This means that the random walk is uncorrelated, such that 'memory' effects are absent and the direction of movement is completely independent of the previous directions moved (Weiss, 1994). Under these assumptions, the corresponding movement type is known as a simple random walk. The probability distributions for the step length λ and turning angle ψ reads,

$$\lambda(l;\sigma) = \frac{l}{\sigma^2} \exp\left(-\frac{l^2}{2\sigma^2}\right), \quad \psi(\theta) = \frac{1}{2\pi} \quad l > 0,\ -\pi < \theta \leq \pi, \tag{2.1.1}$$

where λ is the Weibull[1] distribution with scale parameter $\sqrt{2}\sigma$ and the turning angle is uniformly distributed over the circle, so that each insect has an equal chance of moving in all directions. A simple derivation of how these can be derived from the distributions of (ξ_i, η_i) can be found in Petrovskii et al. (2014).

2.2 Correlated Random Walk (CRW)

More realistic than completely random movement, one would expect insects to maintain a similar direction that coincides with the direction of motion at the previous step - resulting in a short term localized bias referred to as forward persistence (Bovet and Benhamou, 1988). As a result, any two subsequent steps in the random walk are correlated, and the corresponding movement is known as the CRW (Codling et al., 2008). Such mechanisms are ensured if the frequency of large turning angles is suppressed with low probability of occurrence (Bergman et al., 2000). From a modelling perspective, the probability distribution for the turning angle ψ is no longer uniform, and now takes the form of a circular distribution. In this study, we consider the following

$$\lambda(l;\nu) = \frac{l}{\nu^2}\exp\left(-\frac{l^2}{2\nu^2}\right), \quad \psi(\theta;\kappa) = \frac{e^{\kappa\cos\theta}}{2\pi I_0(k)}, \quad l>0,\ -\pi<\theta\leq\pi,\ \nu,\kappa>0, \tag{2.2.1}$$

where λ is the Weibull distribution with scale parameter $\sqrt{2}\nu$ (as in the case of BM), and ψ is the von Mises distribution (VMD) with concentration parameter κ and zero mean (Morales et al., 2004). Note that, other potential candidates for ψ are also suitable e.g. wrapped Cauchy distribution (Fisher, 1995). Here, $I_0(k)$ denotes the zeroth order modified Bessel function of the first kind, defined through the integral $I_0(\kappa) = \frac{1}{2\pi}\int_{-\pi}^{\pi} e^{\kappa\cos\theta}d\theta$. Larger values of κ corresponds to higher concentration, resulting in stronger forward persistence, and vice versa. In the limiting case $\kappa \to 0$, the VMD converges to the uniform distribution, and reduces to the special case of BM if $\kappa = 0$. For simulation methodology, random turning angles centered at each heading θ_i are generated by the relation $\theta_{i+1} = \text{VMD}(\theta_i, \kappa), \theta_0 = 0$. See Fagan and Calabrese (2014) for a contextualization of the CRW and its development within the 'rise of movement ecology'.

2.3 Lévy Walk (LW)

Much discussion in the literature has led to the introduction of an alternative movement pattern known as the Lévy walk (LW). The main difference is that the end tail of the step length distribution decays slowly

[1]The general form for the Weibull distribution is $\lambda(l;\alpha,\beta) = \frac{\alpha}{\beta}\left(\frac{l}{\beta}\right)^{\alpha-1}\exp\left(-\left(\frac{l}{\beta}\right)^{\alpha}\right), l>0$. The step length distribution in (2.1.1) has specific distribution parameters $\alpha = 2$, $\beta = \sqrt{2}\sigma$.

according to a power law ('fat tails'), in contrast to faster than exponential decay for BM ('thin tails'), see (2.1.1). The statistical consequence is that the variance is divergent and the characteristic scale is undefined (scale-free), often regarded as the 'fingerprint' of a LW. The movement path is composed of multiple short steps in clusters with the occasional longer steps in between them, and the resulting movement pattern is much faster. The step length distribution λ is expressed through its asymptotic property, and described by

$$\lambda(l) \sim l^{-\mu}, \quad 1 < \mu \leq 3, \tag{2.3.1}$$

where μ is the tail index. This is undefined for $\mu \leq 1$, since it cannot be normalized and for $\mu > 3$, the end tail decays sufficiently fast, converging to a normal distribution due to the central limit theorem (CLT), and thus the interval of interest is precisely that in (2.3.1). As a technical note, the terminology '*Lévy flight*' or '*Lévy walk*' is synonymous in the biological literature, but a clear distinction is made in the physical sciences, these subtleties are mentioned in Appendix S3. Any subsequent results and analysis that follow actually apply indirectly to LWs. In the ecological literature, there is ample evidence that the movement pattern for a range of animals can be modelled well by the LW (Reynolds, 2012; Focardi et al., 2009; Humphries et al., 2010) and many others, albeit, somewhat controversial since some studies have been contested due to both empirical and theoretical issues being identified (Edwards et al., 2007; Codling and Plank, 2011; Palyulin and Metzler., 2014). Often, the strongest evidence appears in context specific scenarios e.g. optimal searching strategies in resource scarce environments (Bartumeus and Catalan, 2009; Viswanathan et al., 1999). Our motivation for including LWs, stems from the fact that such movement mechanisms are becoming increasingly important and often discussed, more generally, in the context of animal movement.

In principle, we can make use of any type of LW with reasonable choice of μ. For the purposes of this study, we consider a particular example of such, where step lengths are Folded-Cauchy distributed,

$$\lambda(l;\gamma) = \frac{2\gamma}{\pi(\gamma^2 + l^2)}, \quad l > 0, \quad \psi(\theta) = \frac{1}{2\pi}, \quad -\pi < \theta \leq \pi, \tag{2.3.2}$$

with scale-parameter γ and tail index $\mu = 2$, which determines the rate of decay in the end tails i.e. $\lambda \sim \frac{1}{l^2}$. This is an interesting special case due to its ecological significance (e.g. foraging theory), as the corresponding distribution of flight lengths provides an optimal searching strategy under some additional conditions (Viswanathan et al., 1999). The turning angle is uniformly distributed over the circle, and the model is uncorrelated, which occurs in an isotropic environment, assuming the absence of any global or localized bias. Note that, if ψ were some type of circular distribution then the above would describe a correlated Lévy walk (CLW), which is not considered in this paper. For a comprehensive review, see

Reynolds (2018) which discusses in more detail, the 'current status and future directions of Lévy walk research'.

3 Simulation setting

To simulate the pitfall trapping process, consider N individuals homogeneously distributed[2] within a confined arena in the presence of a single trap installed. The movement of each individual is modelled by the random walk, as outlined in §2.1, whilst considering separately BM, CRW and the LW as distinct movement types. Assuming that the system has no immigration/migration properties so that the arena boundary is impenetrable, and the absence of reproduction or mortality (births/deaths), then the total population N can only decrease over time as a result from trapping. The absorbing trap boundary functions in the following way: at any instant in time, if the position $\mathbf{r}_i$ of any individual is located within the trap, then this individual is removed from the system (Petrovskii et al., 2012). It follows that the conservation relation between population number $N(t)$ (number of individuals which remain within the system) and trap counts $J(t)$ accumulated from time $t = 0$ to t is $N(t) + J(t) = N$. In case the individual will 'hit' the trap, so that the position is located precisely on the trap boundary (or close to it), then it is possible to move away from the boundary at the next step, due to a possible re-orientation. This reflects on what is observed in real field tests, since only a low proportion of contacts results in catches, i.e. direct interaction with the trap boundary does not ensure that the insect is trapped (Halsall and Wratten, 1988). Intuitively, we expect that the interplay between trap shape and movement behaviour will affect trap counts and therefore the catch probability. Note that, the movement process described here is a 'jump process' since individuals appear at positions $\mathbf{r}_i$ at times t_i but do not move along the intermediate paths, and so can potentially jump over the traps. This modelling artefact is a minor issue since we know that trap counts computed in this way, correspond well with mean field solutions (Ahmed, 2015).

3.1 Trap geometry

We consider a single trap installed at the centre of a circular arena of radius $r = R_2$, with the following shapes, in separate scenarios.

1. Circular trap with trap radius R_1 ($R_1 < R_2$), perimeter $P = 2\pi R_1$, with trap boundary

$$\partial\Omega_c = \{(r,\theta) : r = R_1,\ -\pi < \theta \leq \pi\}, \tag{3.1.1}$$

[2]See Appendix S1 which describes the simulation methodology for the initial condition. In case of circular geometry the total population is uniformly distributed on an annulus, however, in other square/slot geometries it can be more complicated.

and arena

$$\Omega_c = \{(r,\theta) : R_1 < r < R_2, -\pi < \theta \leq \pi\}. \tag{3.1.2}$$

2. Square trap with (base) length E, width $w = E$, $P = 4E$, with trap boundary

$$\partial\Omega_s = \left\{(x,y) : |x| < \frac{1}{2}E,\ y = \pm\frac{1}{2}E \cap |y| < \frac{1}{2}E,\ x = \pm\frac{1}{2}E\right\}, \tag{3.1.3}$$

and arena

$$\Omega_s = \left\{(x,y) : x^2 + y^2 < R_2^2 \cap |x| > \frac{1}{2}E \cap |y| > \frac{1}{2}E\right\}. \tag{3.1.4}$$

3. Slot trap with length E, width $w = \omega E$, $P = 2E(1+\omega)$, with trap boundary

$$\partial\Omega_\omega = \left\{(x,y) : |x| < \frac{1}{2}E,\ y = \pm\frac{1}{2}\omega E \cap |y| < \frac{1}{2}\omega E,\ x = \pm\frac{1}{2}E\right\}, \tag{3.1.5}$$

and arena

$$\Omega_\omega = \left\{(x,y) : x^2 + y^2 < R_2^2 \cap |x| > \frac{1}{2}E \cap |y| > \frac{1}{2}\omega E\right\}. \tag{3.1.6}$$

Here, c, s, ω are labels referring to the circle, square, and slot geometries, respectively. ω is the aspect ratio between the width and length of the slot, which corresponds to a square trap if $\omega = 1$.

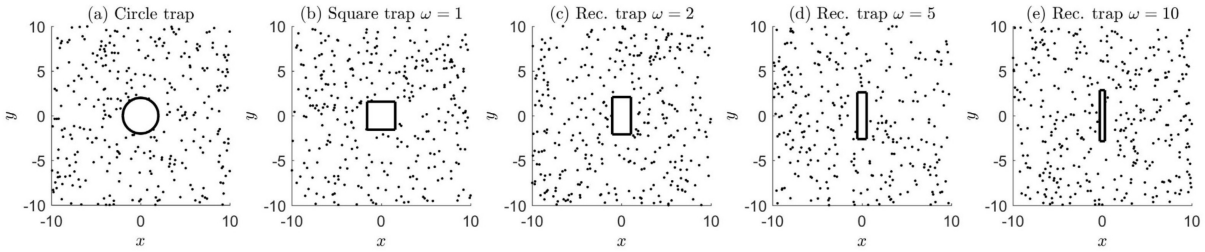

Figure 3.1.1: Trap dimensions: (a) Circular trap with radius $R_1 = 2$ and perimeter $P = 2\pi R_1 = 4\pi$. (b) Square trap $\omega = 1$, with length $E = \pi$, width $w = E = \pi$. (c) Slot trap $\omega = 2$, with $E = \frac{2\pi}{3}$, width $w = \frac{4\pi}{3}$. (d) Slot trap $\omega = 5$, $E = \frac{\pi}{3}, w = \frac{5\pi}{3}$. (e) Slot trap $\omega = 10$, $E = \frac{2\pi}{11}, w = \frac{20\pi}{11}$. All traps have the same fixed perimeter. The initial population distribution is homogeneous, see Appendix S1, and confined within an arena of radius $R_2 = 20$. Only part of the arena is shown here for visual purposes.

Fig. 3.1.1 illustrates the trap dimensions of different trap shapes placed at the centre of the arena, so that the intersection of the lines of symmetry coincide with this point. The geometry is rotationally symmetric with respect to the spatial population distribution, that is, on average, we expect that similar trap counts are obtained if traps were to be rotated. Fig 3.1.1 (b) - (e) shows the transition from square to slot, which is characterized by the aspect ratio ω. As ω increases from 1, the length decreases and width increases, forming a thinner slot with smaller area.

3.2 Arena boundary condition

Once a trap is installed, the trap boundary introduces a perturbation into the population distribution in the vicinity of the trap, and the 'radius' of such a perturbation grows with time. Since the primary interest of insect monitoring is on the short time dynamics, and given that on such a time-scale, the density further away from the trap is essentially unperturbed, it follows that the actual choice of arena shape is not so important, and it is expected that this outer boundary will have negligible effect on trap counts, if any. From a modelling perspective, the arena shape is chosen to avoid unnecessary complications, and obvious choices are either circular or square, depending on the type of co-ordinate system one adopts. Without loss of generality, we consider a fixed circular arena boundary of radius R_2, with perimeter $P_{\text{Arena}} = 2\pi R_2$ and area $A_{\text{Arena}} = \pi R_2^2$. Typically, the ratio between arena and trap scales in a real-field is considerably large, at least one order of magnitude, and the dimensions chosen in our simulations should reflect this. Henceforth, we set arena to trap perimeter ratio as $\frac{P_{\text{Arena}}}{P_{\text{Trap}}} = 10$ times as large, which is sufficient. In case of a circular trap, this means that the arena radius is 10 times trap radius, so that $R_2 = 10R_1$.

The boundary condition for the impenetrable arena boundary can be specified in a number of ways. The common types are; (i) Reflective: angle of reflection is the same as the angle of incidence, (ii) Stop-go or 'sticky': individual remains at the boundary at that meeting point, (iii) No-go: alternative path is chosen at the previous step to ensure individual remains within the arena (Bearup and Petrovskii, 2015). These conditions are quite easy to implement for boundaries with straight edges (e.g. square type), however, for a circular arena, it is best to introduce the concept of a 'projection', defined in the following way: if any individual position is located outside the arena at the i^{th} step, then the individual is projected back onto the arena boundary in the direction of $\mathbf{r}_i$, so that, if $|\mathbf{r}_i| > R_2$ then $\mathbf{r}_i^{\text{new}} = R_2 \cdot \frac{\mathbf{r}_i}{|\mathbf{r}_i|}$, see Fig. 3.2.1 Path B. At the next step, if the position is within the confines of the arena, then the movement process continues as per the random walk model (2.0.1). Over the course of the movement track, the individual may attempt to overstep the arena boundary on multiple occasions, at which point it will always be projected back, in the same manner. This concept is similar in essence to the sticky type condition. Fig. 3.2.1 illustrates typical movement paths to demonstrate the trap function (Path A), and how the actual position is redefined via a projected boundary encounter (Path B).

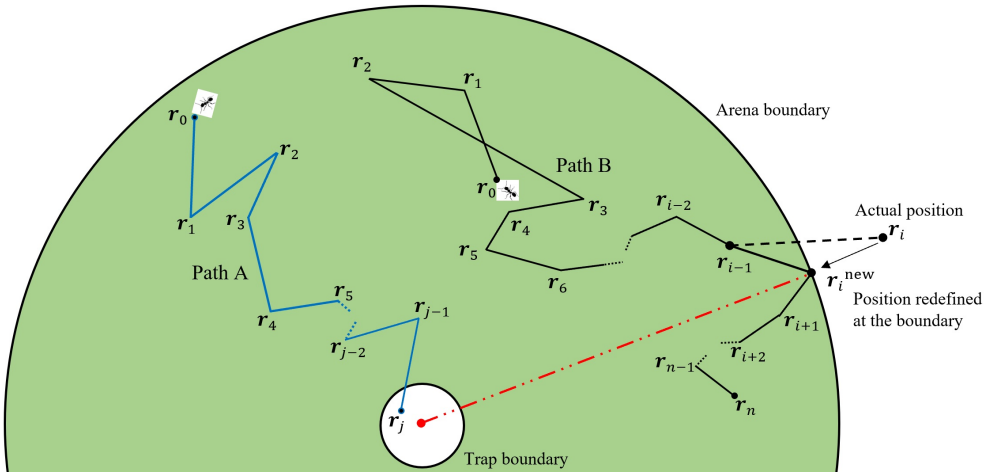

Figure 3.2.1: Illustration of typical movement paths in the case of circular trap geometry. The insect begins at initial position $\mathbf{r}_0$ at time $t = 0$, and further positions are determined by the random walk model (2.0.1). Path A demonstrates the trap function. Insect falls into the trap at the j^{th} step, and is then subsequently removed from the system, forming a trap count. Path B demonstrates the projected boundary encounter. Insect attempts to overstep the boundary at the i^{th} step, and is then projected back onto the arena boundary in the direction of $\mathbf{r}_i$ with new position $\mathbf{r}_i^{\text{new}} = R_2 \cdot \frac{\mathbf{r}_i}{|\mathbf{r}_i|}$.

3.3 Equivalent geometries

At first sight, one may expect that trapping efficiencies are related to the area of the trapping region. Considering those dimensions in Fig. 3.1.1, it is readily seen that the area of the square trap $A_s = \pi^2$ is less than that of the circular trap $A_c = 4\pi$, which can mistakenly be translated to the square trap being less efficient. Under this guise, it may seem that efficiencies are 'self-evident', but on the contrary it is counter intuitive. Trap shapes should actually be compared on a basis of equal perimeter lengths, which is well supported by theoretical, empirical and simulated results (Luff, 1975; Work et al., 2002; Miller et al., 2015). Intuitively, this makes more sense, since trapping is fundamentally a phenomenon of interactions with the trap boundary.

To compare trap efficiencies across different geometries there are two fundamental parameters that must be fixed, firstly, the trap perimeter length P must be the same, from which we can relate trap dimensions

$$E = \frac{\pi R_1}{1+\omega}. \tag{3.3.1}$$

Secondly, the population density ρ (number of individuals per unit area) must be constant. For different trap geometries, this can be ensured by either, fixing the arena size R_2 and varying the total population N, or alternatively, fix N and vary R_2. In this study we adopt the former, but confirm that any loss/gain in area due to varying arena size has negligible effect on captures, irrespective of the type of movement

process or varied insect activity. The two approaches are equivalent, provided that the arena is of a similar size, otherwise, arena boundary encounters can noticeably impact trap counts. On assuming constant population density $\rho = \frac{N_c}{A_c} = \frac{N_\omega}{A_\omega}$, we obtain a relation between population numbers

$$N_\omega = N_c \frac{1 - \frac{\pi\omega}{(1+\omega)^2} \cdot \left(\frac{R_1}{R_2}\right)^2}{1 - \left(\frac{R_1}{R_2}\right)^2}. \tag{3.3.2}$$

If the details in the circular case are specified i.e. circular trap radius R_1 and total population N_c, then corresponding parameters for the equivalent square/slot geometry can be computed using (3.3.1) and (3.3.2) whilst considering different aspect ratios ω.

4 Results

4.1 Impact of trap geometry for Brownian Motion

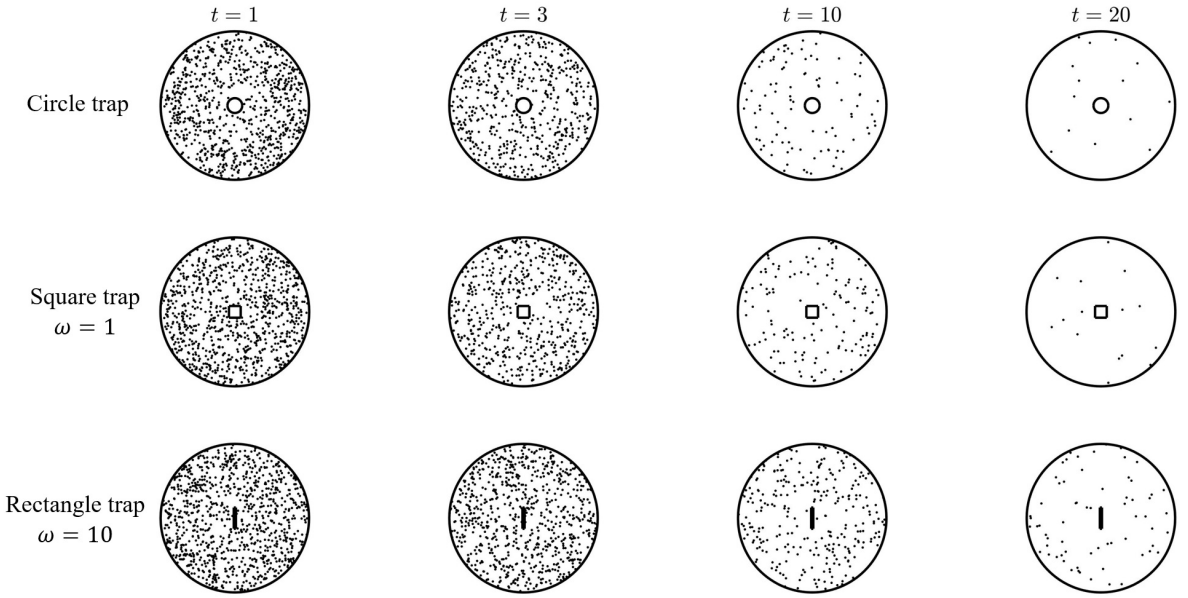

Figure 4.1.1: Snapshots of the spatial distribution with position $\mathbf{r}_i$ shown at times $t = 1, 3, 10, 20$, with corresponding total number of steps $n = 100, 300, 1000, 2000$. (i) Circle trap: Population $N_c = 1244$, trap radius $R_1 = 2$. (ii) Square trap: Population $N_\omega = 1247$, side length $E = \pi \approx 3.14$, aspect ratio $\omega = 1$. (iii) Slot trap: Population $N_\omega = 1253$, length $E = \frac{2\pi}{11} \approx 0.57$, width $w = \frac{20\pi}{11} \approx 5.71$, $\omega = 10$. Other parameters include: time increment $\Delta t = 0.01$, mobility rate $\sigma = 1.5$, arena radius $R_2 = 20$, constant population density $\rho \cong 1$, fixed perimeter $P = 4\pi \approx 12.57$.

Fig. 4.1.1 illustrates the evolution of the spatial distribution at times $t = 1, 3, 10, 20$. The movement process is Brownian with step lengths and turning angles given by (2.1.1). Individuals are uniformly distributed across each arena, with impenetrable arena boundary due to the projection condition. The trap dimensions here are precisely those shown in Fig. 3.1.1, for different trap geometries; circle, square ($\omega = 1$), thin slot ($\omega = 10$), and for brevity the cases $\omega = 2, 5$ are not shown here. On comparing population numbers at $t = 20$, it is clear that details of trap shape has an impact on trapping efficiency.

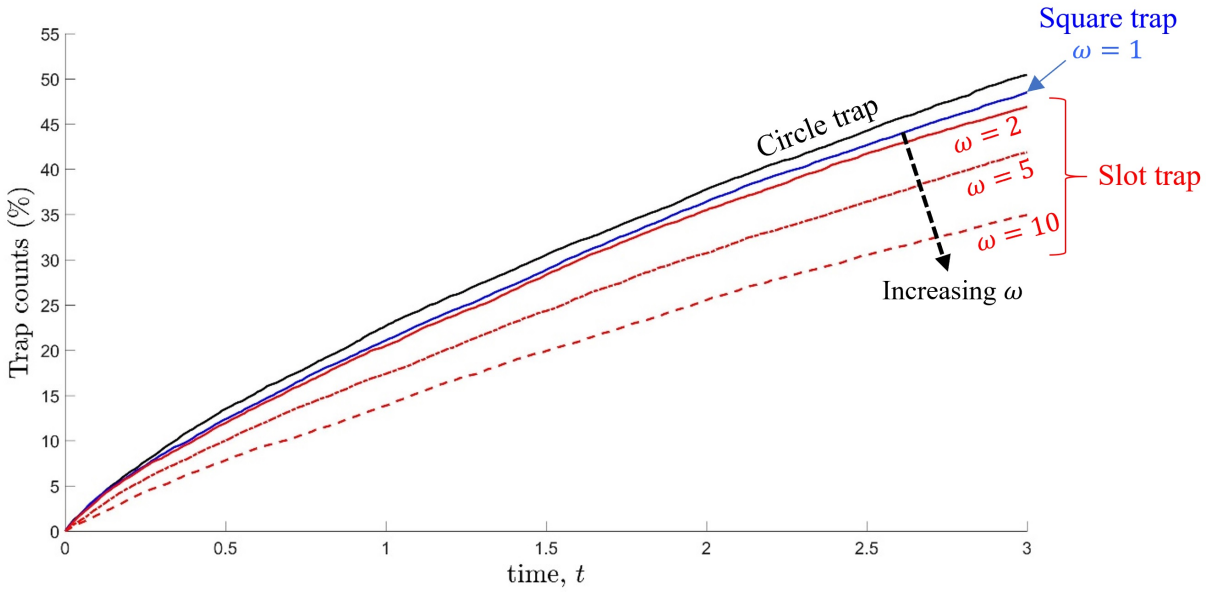

Figure 4.1.2: Trap counts (%) vs time $(t = 0, 0.01, 0.02, ..., 3)$. Trap geometries considered; circle, square $\omega = 1$ and slot $\omega = 2, 5, 10$. Details for the slot trap, include: (i) $\omega = 2$, population $N_\omega = 1248$, length $E = \frac{2\pi}{3} \approx 2.09$, width $w = \frac{4\pi}{3} \approx 4.19$. (ii) $\omega = 5$, population $N_\omega = 1251$, length $E = \frac{\pi}{3} \approx 1.05$, width $w = \frac{5\pi}{3} \approx 5.24$. All other cases with corresponding details are the same as in the caption of Fig. 4.1.1, see also Fig. 3.1.1.

Fig. 4.1.2 compares trap count trajectories across different geometries; circle, square and slot. Since the population is confined and can only reduce as a result of trapping, the trap count trajectories are monotonously increasing, subject to inherent stochastic fluctuations due to the randomness of individual movement. These trajectories are averaged over 20 simulation runs to reduce this effect. The result in Fig. 4.1.2 shows that the circle trap is the most efficient. A small but noticeable difference is observed on comparing to the square trap. In the case of slot geometry a more prominent difference is noticed, with less trap counts recorded as the aspect ratio ω increases, that is, as the slot becomes thinner, see Fig. 3.1.1 (c) - (e). This poorer efficiency in capture rates can be explained by the fact that, insects moving orthogonally to the shortest sides will, on average, outweigh the gains from the longest sides. It is evident that there is a hierarchy of trap shapes with respect to impacts on trap efficiency, with trap count differences growing with time.

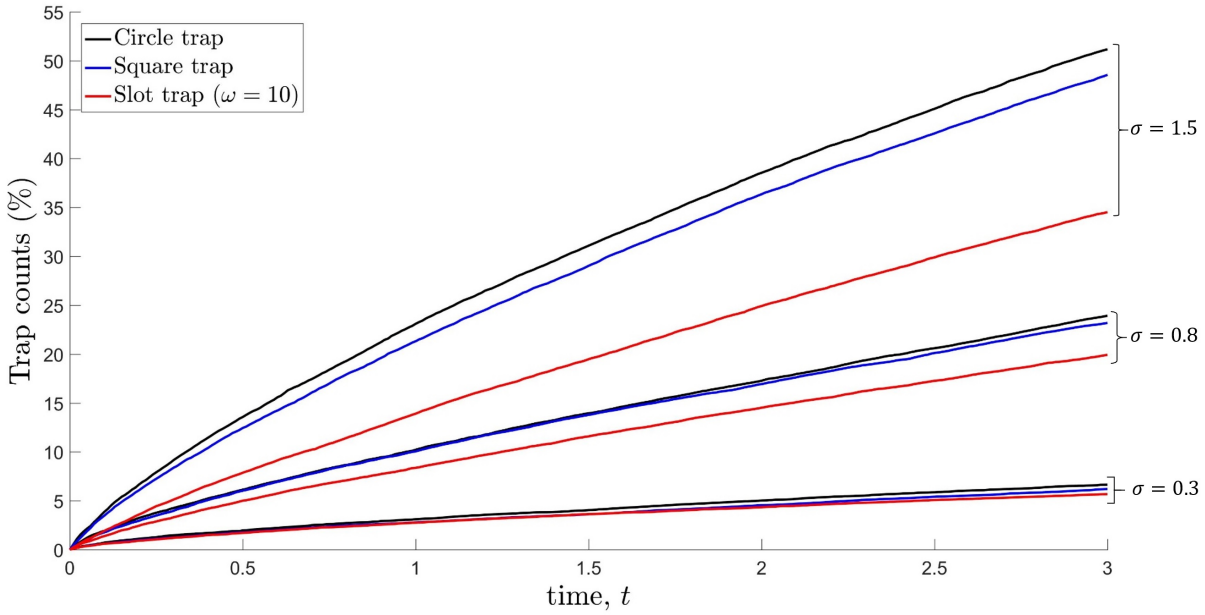

Figure 4.1.3: Trap counts (%) vs time $(t = 0, 0.01, 0.02, ..., 3)$ for varying mobility rates $\sigma = 0.3, 0.8, 1.5$. Trap geometry: (i) Circle trap: Population $N_c = 1244$, trap radius $R_1 = 2$. (ii) Square trap: Population $N_\omega = 1247$, length $E = \pi \approx 3.14$, ratio parameter $\omega = 1$. (iii) Thin slot trap: Population $N_\omega = 1253$, length $E = \frac{2\pi}{11} \approx 0.57$, width $w = \frac{20\pi}{11} \approx 5.71$, $\omega = 10$. Other details include: time increment $\Delta t = 0.01$, arena radius $R_2 = 20$, population density $\rho \cong 1$, perimeter $P = 4\pi \approx 12.57$.

Fig. 4.1.3 shows that the most efficient trap is the circular, square, and then slot, in this precise order, even in the case of varied mobility (insect activity) - where trap count differences are more realised for larger mobility rates. To quantify this 'impact', we introduce the following: firstly, denote $J^m(i\Delta t),\ i = 1, 2, ..., n$ as the accumulated trap count recorded after i steps, with time step Δt and total duration of trap exposure $T = n\Delta t$. The index m denotes the m^{th} recording, which serves as a counter for multiple simulation runs, synonymous to repeated experimental trials in the real field. Let $\hat{J}^m = \frac{J^m}{N}$ denote the total number of individuals trapped 'normalized' by total population. Normalization is required since the total population varies across different geometries to ensure constant population density. We can then compute the 'relative' normalized trap counts $\Delta\hat{J}^m$ between circular and other geometries,

$$\Delta\hat{J}^m(i\Delta t) = \frac{J_c^m(i\Delta t)}{N_c} - \frac{J_\omega^m(i\Delta t)}{N_\omega}. \tag{4.1.1}$$

Recall that $\omega = 1$ corresponds to the square trap, and $\omega > 1$ for slot traps. If $\Delta\hat{J}^m$ is positive then the normalized trap count is greater in the circular geometry, vice versa if negative, and the same if equal to

zero. On averaging over M simulation runs and n steps, we obtain the simple statistical metric

$$\left\langle \Delta\hat{J} \right\rangle = \frac{1}{nM} \sum_{i=1}^{n} \sum_{m=1}^{M} \Delta\hat{J}^m(i\Delta t) = \frac{1}{nM} \sum_{i=1}^{n} \sum_{m=1}^{M} \left(\frac{J_c^m(i\Delta t)}{N_c} - \frac{J_\omega^m(i\Delta t)}{N_\omega} \right), \tag{4.1.2}$$

which provides a means to quantify the 'impact of trap geometry' through normalized trap count differences. It is expected that this metric should complement any conclusions drawn from qualitative comparisons of trap count trajectories.

Mobility rate σ	$\left\langle \Delta\hat{J} \right\rangle$ (%)	
	Square vs. Circle	Slot ($\omega = 10$) vs. Circle
0.3	0.38	0.52
0.8	0.28	2.99
1.5	1.85	10.73

Table 4.1.1: Relative normalized trap counts averaged over $n = 300$ steps and $M = 20$ simulation runs $\left\langle \Delta\hat{J} \right\rangle$. The metric is computed for varying mobility rates.

Tab. 4.1.1 shows that in the case of square vs. circle, with low mobility rates such as $\sigma = 0.3, 0.8$, the value of the metric $\left\langle \Delta\hat{J} \right\rangle$ is of the same order and less than 1%, and therefore, trap shape does not have much impact. In the slot vs circular case, $\left\langle \Delta\hat{J} \right\rangle$ increases from 0.5% to 3% approx - indicating that slot type traps are significantly less efficient. For larger mobility rates such as $\sigma = 1.5$, the value of $\left\langle \Delta\hat{J} \right\rangle$ is relatively greater, more so in the case of slot geometry. This means that details of trap shape such as impact of corners is important, but largely depends on insect activity, with greater impacts registered for faster moving insects.

It is well known that the spatio-temporal population density $\rho(\mathbf{r}, t)$ of a system of individuals performing BM with diffusion rate D is a solution of the diffusion equation (Berg, 1983; Sornette, 2004)

$$\frac{\partial \rho}{\partial t} = D \left(\frac{\partial^2 \rho}{\partial x^2} + \frac{\partial^2 \rho}{\partial y^2} \right), \tag{4.1.3}$$

which can easily be derived from a simple random walk (Codling et al., 2008). The hallmark of BM is that the mean squared displacement (MSD) grows linearly with time, which yields a relation between the mobility rate σ and D, written $\sigma^2 = 2Dt$ (Turchin, 1998). For a discrete time model, one can expect that this remains valid, at least approximately, for a small, but finite value of Δt, that is

$$\sigma^2 = 2D\Delta t. \tag{4.1.4}$$

In some simple cases, analytical solutions for the diffusion equation (4.1.3) can be found, subject to appro-

priately chosen initial and boundary conditions. For instance, a solution can be sought as an infinite series in the case of circular trap geometry with uniform initial density, but not useful, because the coefficients in the series contain zeros of Bessel functions that are not known analytically and must be computed numerically (Carslaw and Jaeger, 1959). In other more complex geometries such as the case of square/slot trap geometry, analytical solutions do not exist, and therefore one must resort to numerical techniques anyway (Strauss, 2008).

Petrovskii et al. (2012) studied trap efficiency between the circular and square cases, by computing the numerical solution to the diffusion equation (4.1.3) and comparing the flux through the trap boundary, over the time interval $0 < t < 3$. It was deduced that trap counts do not depend much on the details of the trap shape, and thus the impact of corners in case of square geometry is not important. The results showed that the circle trap was slightly more efficient, but the difference was far too negligible to suggest otherwise. Here, the flux was compared with fixed diffusion coefficient $D = 1$, and for fixed time increment $\Delta t = 0.01$ (as used in Fig. 4.1.3), which corresponds to a mobility rate $\sigma = \frac{\sqrt{2}}{10} \approx 0.141$, calculated from (4.1.4). This value of σ is far too low (c.f. Fig. 4.1.3), to observe any considerable changes in trap counts, also, see Tab. 4.1.1 square vs. circle, where $\langle \Delta \hat{J} \rangle$ is well below 1%. Although the claim can be substantiated for these chosen parameters or other cases of low mobility, our results demonstrate that this conclusion is not necessarily true for ground-dwelling arthropods which are highly active. Trap shape can indeed affect the efficiency of trap counts, but only noticeable provided the mobility rate $\sigma \sim \sqrt{Dt}$ is sufficiently large.

In relation to observations in the real field, relatively lower mobility rates are typically reported for a variety of taxa, e.g. the lady beetle (*Epilachna sparsa orientalis*) $\sigma = 0.12$ $(D = 0.71)$ (Iwao and Machida, 1963), native tree hopper (*Publica concava*) $\sigma = 0.07$ $(D = 0.23)$ (McEvoy, 1977), leaf beetle (*Galerucella pusilla* and *Galerucella calmariensis*) $\sigma = 0.10$ $(D = 0.46)$ (Grevstad and Herzig, 1997). These diffusion coefficients D are recorded in these texts (measured in $\mathrm{m}^2/\mathrm{day}$), but have been converted to σ using (4.1.4) with $\Delta t = 0.01$, as used in our simulations. There is empirical evidence that insect activity can depend on habitat structure, for example, the meta-analysis by Allema et al. (2015) showed that mobility rates of Carabid beetles (*Carabidae*) is approximately 5.6 times as high in farmland as in woody habitat. In particular, those species associated with forested habitats had greater mobility than those associated with open field habitats, both in arable land and woody habitat. In case of forested habitat with arable land, σ is observed to typically vary between $[1.29, 2.63]$ $(D = [83, 347])$. The implication is that, impacts of trap geometry may be magnified in specific habitats, particularly where ground-dwelling arthropods are known to exhibit faster movement.

4.2 Impact of trap geometry for non-Brownian Motion

To compare between two distinct movement processes, scale parameters must be related by some type of 'condition of equivalence'. In case of BM and the CRW this can be done easily, as both are scale-specific processes, and a relation can be sought by equating the mean squared displacement (MSD) (Kareiva and Shigesada, 1983). Appendix S2 provides a derivation of the result

$$\nu = \sigma \left\{ 1 + \frac{\pi}{2} \cdot \frac{\frac{I_1(\kappa)}{I_0(\kappa)}}{1 - \frac{I_1(\kappa)}{I_0(\kappa)}} \left(1 - \frac{1}{n} \cdot \frac{1 - \left(\frac{I_1(\kappa)}{I_0(\kappa)}\right)^n}{1 - \left(\frac{I_1(\kappa)}{I_0(\kappa)}\right)} \right) \right\}^{-\frac{1}{2}} \tag{4.2.1}$$

which relates the CRW distribution parameter ν in terms of the mobility parameter σ for BM, after n steps, given some concentration κ. If $\kappa = 0$, then the CRW reduces to BM with $\nu = \sigma$, as expected. $I_0(k)$ and $I_1(k)$ are defined through the integral $I_p(\kappa) = \frac{1}{2\pi}\int_{-\pi}^{\pi} \cos(p\theta) e^{\kappa \cos\theta} d\theta$, which denotes the p^{th} order modified Bessel function of the first kind.

Since LWs are essentially scale-free, in the sense that the variance of step lengths is divergent (and therefore so is the MSD), it follows that the usual methodology outlined above cannot be applied. In Appendix S3 we derive a new and unique equivalence condition which can be used, more generally, to relate between any two movement processes when the variance of at least one of them does not exist, based on minimizing the 'distance' in the sense of $\mathscr{L}_2$ norm, between the corresponding step length distributions. In case of BM and the LW with Folded-Cauchy distributed step lengths (2.3.2), we compute the following relation

$$\gamma = 1.536\sigma \tag{4.2.2}$$

where γ is the distribution parameter for the LW. This improves on previously used approaches, where such relations are arbitrarily derived and therefore ambiguous (Rodrigues et al., 2015; Bearup et al., 2016).

Now that the movement mechanisms for the CRW and LW alongside these inter scale parameter relations have been introduced (4.2.1) - (4.2.2), the next step is to analyse how trap catch patterns alter if insect movement behaviour is correlated or of Lévy type.

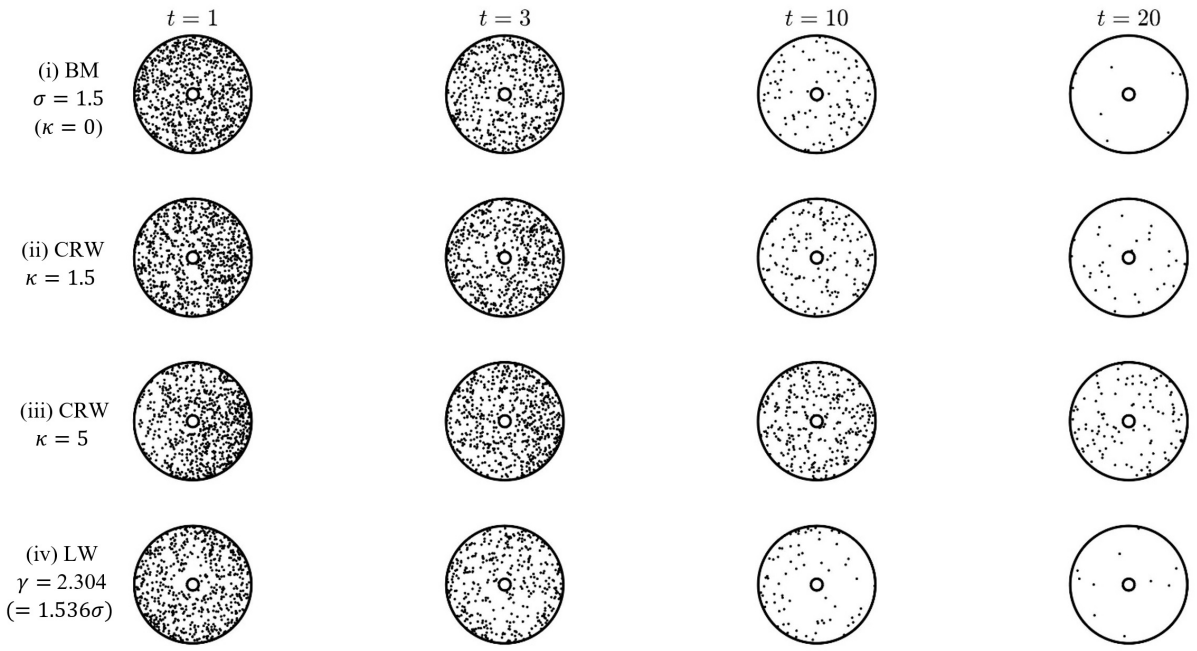

Figure 4.2.1: Snapshots of the spatial distribution in the case of circular trap geometry. Individual position $\mathbf{r}_i$ is shown at times $t = 1, 3, 10, 20$ with corresponding total number of steps $n = 100, 300, 1000, 2000$. The type of movement processes considered are: (i) BM with mobility rate $\sigma = 1.5$ (ii) CRW with low forward persistence $\kappa = 1.5$ (iii) CRW with high forward persistence $\kappa = 5$. In both cases, for the CRW, the mobility rate ν is determined by (4.2.1) (iv) LW with γ found from (4.2.2). Other details: Initial population $N_c = 1244$, trap radius $R_1 = 2$, time increment $\Delta t = 0.01$, arena radius $R_2 = 20$, constant population density $\rho \cong 1$.

Fig. 4.2.1 shows the evolution of the spatial distribution with time, in the case of circular geometry, whilst considering the following movement processes: (i) BM with mobility rate $\sigma = 1.5$, (ii) CRW with low forward persistence $\kappa = 1.5$, (iii) CRW with higher persistency $\kappa = 5$, (iv) LW with $\gamma = 2.304$. For (ii) - (iv) scale parameters are related to the BM case, through the conditions of equivalence (4.2.1) and (4.2.2). For case (iii) CRW for small time, there is a tendency for the individuals to move in the rightward direction, as expected, since the turning angle distribution ψ is centered about $\theta_0 = 0$. On comparing population numbers at $t = 20$, it is clear that the inclusion of forward persistence has an impact on trap captures, with less counts recorded for higher persistency - indicating the importance of movement behaviour. For brevity, the cases of square and slot traps are not shown here - but intuitively, the implications are the same. It is unclear from these snapshots, what impact may result from switching from BM to LW due to similar counts, therefore, further analysis of trap count trajectories is required.

4.2.1 Impact of trap geometry

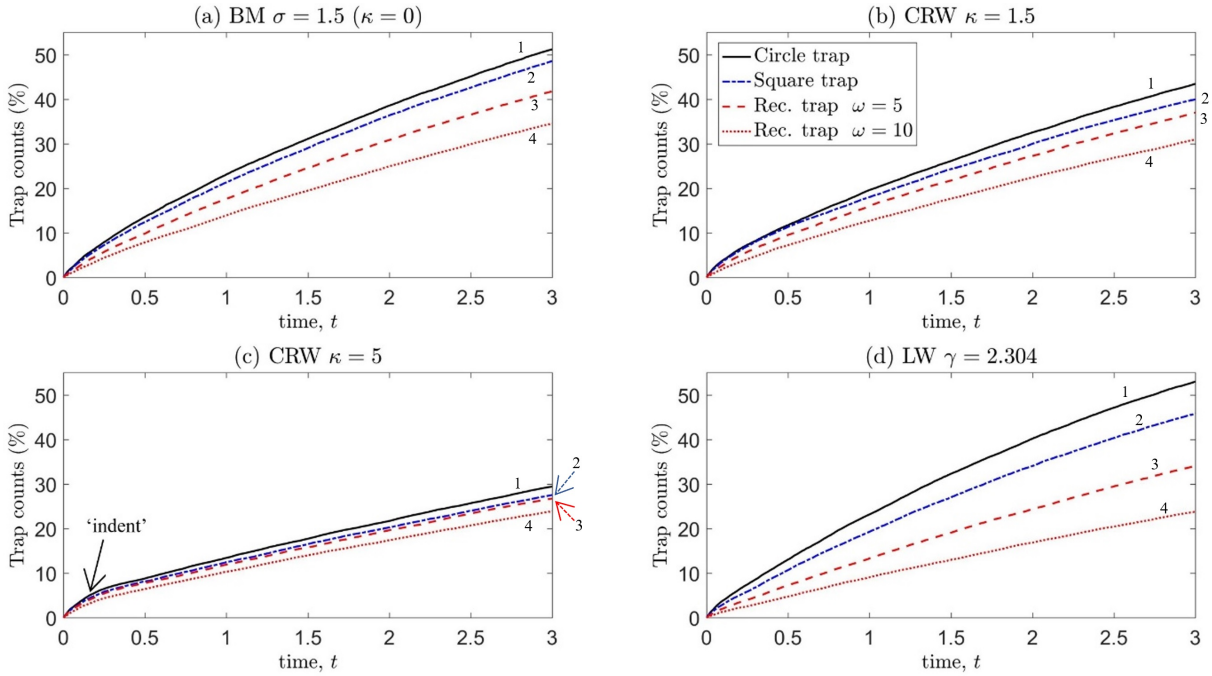

Figure 4.2.2: Trap counts (%) for **different trap geometry**, partitioned by type of movement process: (a) BM with mobility rate $\sigma = 1.5$ (b) CRW with low forward persistence $\kappa = 1.5$ (c) CRW with high forward persistence $\kappa = 5$. In both cases, for the CRW, the mobility rate ν is determined by (4.2.1) (d) LW with γ found from (4.2.2). Trap geometries: circle, square $\omega = 1$ and slot $\omega = 5, 10$. Details of trap dimensions are shown in Fig. 3.1.1. All other details are the same as in the caption of Fig. 4.1.1.

Movement process	$\langle \Delta \hat{J} \rangle$ %		
	Square vs. Circle	Slot ($\omega = 5$) vs. Circle	Slot ($\omega = 10$) vs. Circle
BM $\sigma = 1.5$ ($\kappa = 0$)	1.86	6.18	10.76
CRW $\kappa = 1.5$	1.88	4.19	8.10
CRW $\kappa = 5$	1.25	1.83	3.71
LW $\gamma = 2.304$	4.70	12.10	17.90

Table 4.2.1: Relative normalized trap counts averaged over $n = 300$ recordings and $M = 20$ simulation runs $\langle \Delta \hat{J} \rangle$. These values are listed for different movement processes, each related to the BM case with mobility parameter $\sigma = 1.5$.

Fig. 4.2.2 shows trap count trajectories for different trap geometries, partitioned by type of movement process. On comparing the order of the trajectories in terms of efficiency, we observe that the hierarchy of trap shapes is ranked as: (1) circular, (2) square and then (3) slot $(\omega = 5)$ with less counts recorded for a (4) thinner slot $(\omega = 10)$. Tab. 4.2.1 also confirms this, which lists the values of the statistic

defined earlier in (4.1.2) - since the magnitude of relative normalized trap counts $\langle \Delta \hat{J} \rangle$ increases across each row, irrespective of the movement type. On comparing (a) - (c), we observe that if individuals persist in a localized direction, then the chances of being trapped are lower, as less counts are registered if the movement model is correlated. Also, from Tab. 4.2.1, on the whole, $\langle \Delta \hat{J} \rangle$ decreases with higher forward persistence, which means that the impact of trap geometry is less significant for heavily correlated movement paths. Note that, the 'indent' in the trajectory shown in (c), is a direct consequence of the condition of equivalence as depicted in Appendix Fig. S2.1 (a), since the mobility rate ν reduces and approaches a constant value, see asymptotic relation Appendix (S2.11). Trap counts accumulate rather fast on a short time scale, with a sudden reduction in the rate of accumulation forming such an 'indent', which is more prominent for larger κ. In the case of the LW shown in (d), there is relatively large variation in trap counts for different geometries, also supported by those values in Tab. 4.2.1 (shaded), compare $\langle \Delta \hat{J} \rangle$ with the other cases of BM or CRW. This shows that the impact of trap geometry is more realised when the step length distribution exhibits a slower rate of decay i.e. if the movement pattern allows for occasional large steps. This is a typical example of how theoretical ecology and simulations in particular, can provide information that is sometimes difficult or near enough impossible to obtain from field studies.

4.2.2 Effect of mobility rate

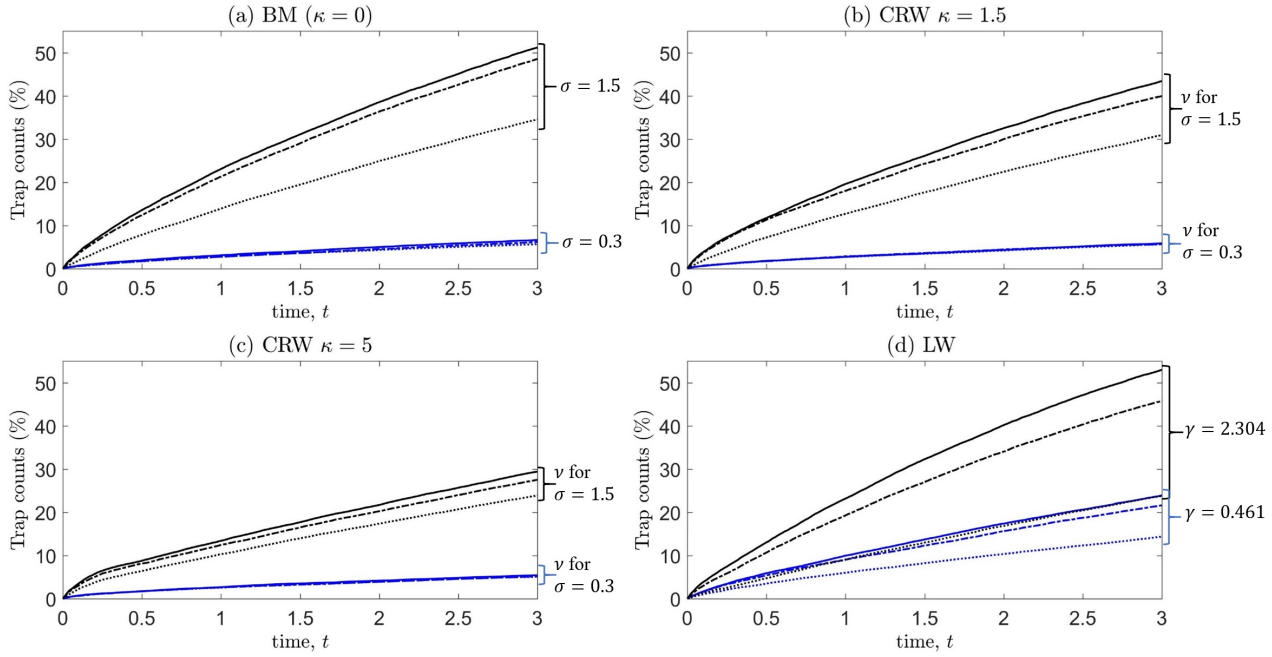

Figure 4.2.3: Trap counts (%) for varying **mobility rates** $\sigma = 0.3$ (black), $\sigma = 1.5$ (blue), partitioned by type of movement process: (a) BM with mobility rate $\sigma = 1.5$ (b) CRW with low forward persistence $\kappa = 1.5$ (c) CRW with high forward persistence $\kappa = 5$. In both cases, for the CRW, the mobility rate ν is determined by (4.2.1) corresponding to each σ (d) LW with γ found from (4.2.2), $\gamma = 2.304$ for $\sigma = 1.5$ and $\gamma = 0.461$ for $\sigma = 0.3$. Trap geometries: circle (solid), square $\omega = 1$ (dashed-dotted) and thin-slot $\omega = 10$ (dotted). Details of trap dimensions are shown in Fig. 3.1.1. All other details are the same as in the caption of Fig. 4.1.1.

Movement process	$\langle \Delta \hat{J} \rangle$ %	
	Square vs. Circle	Slot ($\omega = 10$) vs. Circle
BM $\sigma = 0.3$ ($\kappa = 0$)	0.38	0.52
CRW $\kappa = 1.5$	-0.02	0.10
CRW $\kappa = 5$	0.19	0.17
LW $\gamma = 0.461$	1.26	5.34

Table 4.2.2: Relative normalized trap counts through the trap boundary averaged over $n = 300$ recordings and $M = 20$ simulation runs $\langle \Delta \hat{J} \rangle$. These values are listed for different movement processes, each related to the BM case with mobility parameter $\sigma = 0.3$.

Fig. 4.2.3 demonstrates that the impact of trap geometry is only significant if the mobility rate is sufficiently large, as previously discussed at the end of §4.1. For BM and the CRW, see plots (a) - (c), and low mobility parameter such as $\sigma = 0.3$, the trajectories are almost indistinguishable. This holds whether

the movement paths are correlated or not. Tab. 4.2.2 shows that the relative normalized trap counts is well below 1% (unshaded). The negative recording of $\langle \Delta \hat{J} \rangle = -0.02$ technically means that trap counts are on average greater in the square geometry, however, this difference is far too small and most likely due to stochastic fluctuations. For the LW with $\gamma = 0.461$ (corresponding to $\sigma = 0.3$), there is a noticeable difference in trap counts, see plot (d) and compare to (a) - (c), with considerably larger percentage differences in Tab. 4.2.2 (shaded). This can be explained by the higher frequency of rare but large steps, resulting in a faster movement pattern. In terms of mobility rates, even though γ is conditionally equivalent to σ through (4.2.2), it is still large enough so that the impact of trap geometry is realised. If γ is sufficiently small, then we expect the details of trap shape to have little or almost no impact on trap counts.

4.2.3 Impact due to movement type

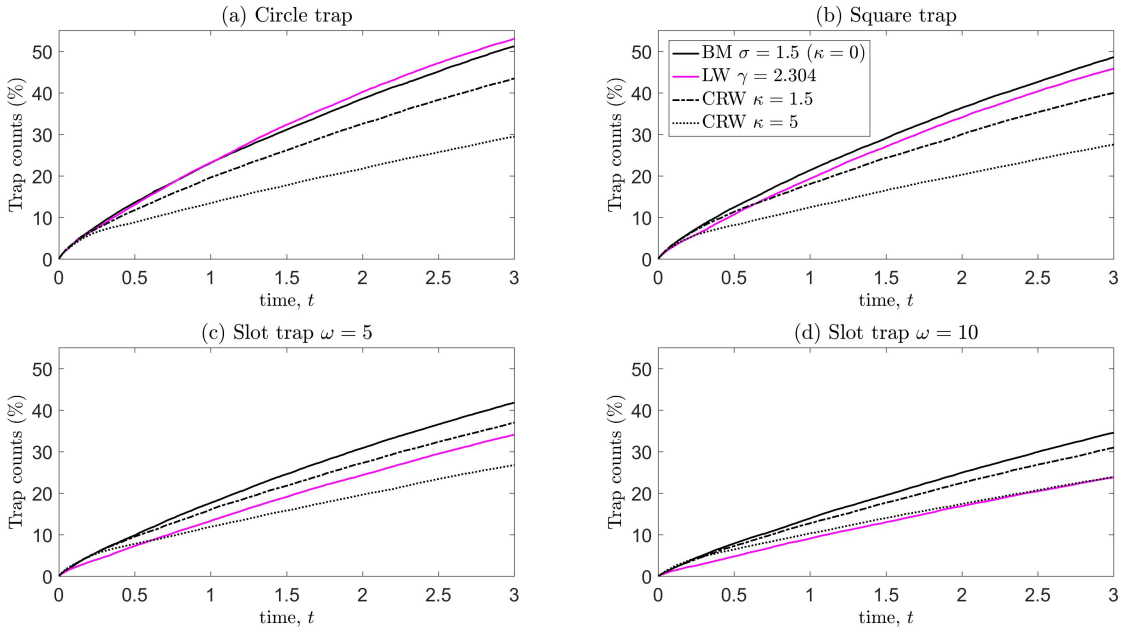

Figure 4.2.4: Trap counts (%) for **distinct movement processes**, partitioned by trap geometry: (a) circular (b) square $\omega = 1$ (c) slot $\omega = 5$ (d) thin-slot $\omega = 10$. Details of trap dimensions shown in Fig. 3.1.1. All other details are the same as in the caption of Fig. 4.1.1.

Trap geometry	$\langle \Delta \hat{J} \rangle_{\mathrm{MP}}\%$		
	CRW ($\kappa = 1.5$) vs. BM	CRW ($\kappa = 5$) vs. BM	LW vs. BM
Circle ($\kappa = 0$)	4.50	12.44	-0.88
Square	4.53	11.83	1.97
Slot ($\omega = 5$)	2.51	8.08	5.04
Slot ($\omega = 10$)	1.84	5.38	6.25

Table 4.2.3: Relative normalized trap counts through the trap boundary averaged over $n = 300$ recordings and $M = 20$ simulation runs $\langle \Delta \hat{J} \rangle$. These values are listed for different movement processes, each related to the BM case with mobility parameter $\sigma = 1.5$.

Fig. 4.2.4 shows trap counts for different movement processes, partitioned by trap geometry. Evidently, capture rates can vary significantly depending on the type of movement behaviour adopted. To quantify this, we can compute the average normalized trap counts (relative to the conceptual case of BM) as

$$\langle \Delta \hat{J} \rangle_{\mathrm{MP}} = \frac{1}{nM} \sum_{i=1}^{n} \sum_{m=1}^{M} \Delta \hat{J}^{m}_{\mathrm{MP}}(i\Delta t) = \frac{1}{nM} \sum_{i=1}^{n} \sum_{m=1}^{M} \left(\frac{J^{m}_{\mathrm{BM}}(i\Delta t)}{N} - \frac{J^{m}_{\mathrm{MP}}(i\Delta t)}{N} \right), \tag{4.2.3}$$

here the label 'MP' refers to the 'movement process', such as CRW or LW, and the total population $N = N_c, N_s$ or N_ω depends on each respective trap shape, as mentioned in the caption of Fig. 4.1.1. Plots (a) - (c) demonstrate that the CRW yields less trap counts in comparison to BM, irrespective of the type of geometry (compare black trajectories), which is exacerbated with greater forward persistence. Note that, the value of $\langle \Delta \hat{J} \rangle_{\mathrm{MP}}$ is magnified across each unshaded row in Tab. 4.2.3 with increasing concentration κ. Moreover, the impact of this movement type is lessened for thinner slots, and in the extreme case of severely elongated slots, it may not matter whether persistence mechanisms are present or not, as demonstrated by the 'overall' decrease in $\langle \Delta \hat{J} \rangle_{\mathrm{MP}}$ unshaded columns. For the LW, the order of trajectories alternate, depicting an irregular pattern, suggesting that trap counts are heavily dependent on details of trap shape. From plot (a) in the case of the circular trap, Lévy walking behaviour yields optimal trap counts, whereas, there is better trapping efficiency with BM in case of square trap geometry. The impact of movement type is more realised for slot traps, and grows for thinner slots, see Tab 4.2.3 shaded column. This is in strict contrast to the CRW vs BM case, where the opposite effect is observed. In summary, the above describes the typical interplay between movement type and trap shape in the context of trapping efficiencies.

5 Summary of results

To summarise, our main findings are as follows:

1. Contrary to the assumption often made in field studies, for e.g. see Blackshaw et al. (2018), slot-shaped traps are significantly less efficient compared to circular or square-shaped traps of the same perimeter. For the same population, the counts obtained with a slot-shaped trap can be more than twice less than the traps obtained with the equivalent circular trap (cf. Fig. 4.2.2). To notice significant impacts of trap shape, we find that insect activity must be large enough, (see Fig. 4.1.3).

2. For a given trap shape, the trap count significantly depends on the type of insect movement but the hierarchy of movement types (i.e. which movement types are trapped more efficiently) can be different for different trap shapes. A general observation is that the rate at which the population is being trapped decreases with an increase in the persistency of the movement (as quantified by parameter κ); in particular, the population of insects performing CRW is trapped at a slower rate compared to the population of insects performing BM (see Fig. 4.2.4). In specific cases, such as for thin slots with movement patterns incorporating low forward persistence mechanisms, the impact on trap counts are somewhat negligible.

3. The rate of trapping of the LW population strongly depends on the trap shape. In case of a circular trap, the populations of LW individuals is trapped at the fastest rate, i.e. providing, on average, the largest trap count. However, in case of a slot-shaped trap, the rate of trapping of the LW population is the lowest, c.f. Figs. 4.2.4 (a) and 4.2.4 (d). For thinner slots, this movement type can severely exacerbate the impact on trap counts, but inconsequential if movement paths are correlated.

These results are primarily based on theory through modelling and simulations, and we hope that other researchers, primarily ecologists and/or entomologists, will be motivated to test these predicted patterns using well selected model species, whilst considering different movement activities, to evaluate them under field or at least laboratory conditions.

6 Discussion

1. In this study, we focused on trapping efficiency of different trap shapes, and how capture rates are affected by movement behaviour, and to what extent. Our results, as outlined in §5, have some broader implications. Traps are widely used for surveying insect diversity, detection of invasive pests and as a form of pest management in agricultural fields (using either e.g. sticky traps, pitfall traps, or alternatively trap crops). In this context, simulation models of insect movement have been used to optimize the spatial distribution and other features of traps, but, the geometry of these structures have hardly ever been assessed on trapping efficiency (Hannunen, 2005). The logic in this study could be applied to determine the optimal physical design of trap systems, which would constitute

an important line of direction for future research work. Also, impacts of trap geometry would be a crucial aspect to be considered, for those who seek to propose a unified trap design (Brown and Matthews, 2016). More generally, a good understanding of the interplay between trap shape, adopted movement types and the subsequent effect on captures, would facilitate better trap count interpretations - which is known to be a challenging issue (Petrovskii et al., 2012).

2. Through simulations, Miller et al. (2015) found that slot traps (line traps) of equal perimeter to have similar or even higher efficiency rates than circular shaped traps. Moreover, capture rates for square traps were shown to be noticeably higher (see §4.5 in that book). Both of these observations apparently contradict with our results, but can be explained with a closer look at the simulation methodology used therein. Some of the issues include: (i) A total number of 5000 random walkers were seeded into an environment, and those individuals happening to originate within the confines of the trap were excluded from the data. The resulting population is less than the original total, and varies due to differences in trap area. Therefore the population density is not constant, which is fundamentally required for comparisons across different geometries (see §3.3). (ii) The movement type used is a Weston random walk[3] with circular standard deviation of 20°, corresponding to a heavily directed movement path with extremely high concentration (relative to those used in this study). We know from Fig. 4.2.2 (a) - (c), that strong correlations can reduce the impact of trap geometry, making trap count trajectories more difficult to differentiate. (iii) Trap counts were simulated for a single simulation run and were not averaged, allowing for considerable stochastic fluctuations. Note that, the simulations conducted by Miller et al. (2015) were designed for a specific goal, that is, to show that catch rates are related to perimeter length. For intricate information, such as comparing trapping efficiencies, much more care must be taken. Taking the above (i) - (iii) into account, we do not see a clear contradiction as our purposes are different.

3. By computing the diffusive flux through boundaries, and on comparing, Petrovskii et al. (2012) showed that the impact of trap geometry is not so important (in the circular vs. square case) - which is correct in case of low insect activity. For substantial differences to be realised, we find that mobility rates must be sufficiently large (see §4.1). If mobility is much smaller than those rates which determine these movement types to be conditionally equivalent, then the impact of trap geometry can possibly be non-existent, even for faster movement types such as the LW. The implication is that for field studies, the choice of trap shape may become important depending on the movement capabilities of the type of species and thus habitat specific, e.g. high dispersal rates

[3]A Weston random walk is a CRW with fixed step length and each new heading is randomly generated from a normal distribution centered on the previous heading. The concentration parameter is defined through the circular standard deviation.

have been recorded for Carabid beetles (*Coleoptera: Carabidae*) in farmland in contrast to lower rates measured in woody habitats, see Tab. 2 in Allema et al. (2015).

4. Capture rates are strongly influenced if the movement paths are correlated, i.e. if insects exhibit memory, such as recollection of previous locations. In such a scenario, trap counts tend to accumulate at a much slower rate. With greater persistency, not only is there a gradual reduction in captures, but also the impact of trap geometry is lessened (see Fig. 4.2.4). In terms of trap data interpretation, low catches can arise due to a multitude of reasons, e.g. low population densities, if abundant food resources are available, due to the biological state of insects such as lack of need for mating, or can even be more complicated, such as a composition of the above. These factors directly influence insect mobility and in turn impact trap counts. We find that, alongside these reasons, the underlying movement mechanisms play a major role in how trap counts are formed, and thus provides an alternative explanation for low counts i.e. if forward persistence is prevalent. To unravel, which of these is 'most' responsible for low counts, is more difficult to answer, and should be the subject of another study. As a starting step, one would need to identify exactly how these factors influence mobility rates and to what extent (Masó, 2015).

5. Many recent studies (but not all) which have reported LW behaviour in animal movement data have been criticized, partly due to usage of inappropriate statistical techniques and misinterpretations of data (Edwards, 2011). In some cases, movement has been incorrectly identified as Lévy type as other movement models produce a similar pattern, such as the composite correlated random walk (CCRW) (Plank and Codling, 2009). In the context of trapping, it was recently shown that almost identical trap counts are reproduced for inherently different movement models, such as BM with time dependent mobility rate and the LW, which suggests that the type of underlying movement pattern is not that important after all, unless placed under some ecological context, e.g. pest monitoring (Ahmed et al., 2018). Although controversy persists, our motivation for including LWs stems from the fact that such mechanistic processes have received much attention in the movement ecology literature (Reynolds, 2018). Our results show that, if animals switch to Lévy type movement (typically observed in resource scare environments), then trap counts strongly depend on trap shape. In the case of circular geometry, optimal trap counts are recorded for a system of Lévy walkers, but for square geometry, BM yields the optimal (see Fig. 4.2.4). This suggests that individuals can avoid portions of the trapping region if corners are present. Intuitively, the frequency of 'avoidance' increases for slot traps, and even more so for thinner slots, possibly a by-product due to a reduction in 'effective size'. Moreover, the impact of trap geometry grows with time, with the opposite effect observed for correlated movement paths with increasing strength of forward persistence. These results have some

wider implications which are applicable, more generally for animal movement. For instance, if we think of the trapping region as a circular area which contains a food patch at the centre, and the trap radius as a detection boundary, then the problem is analogous to random searches. If in addition we assume that any animal which enters the boundary, remains in the close vicinity of the food source (non-revisitable) - then this essentially functions as a 'trapped' individual. In this context, our results agree with the fact that Lévy type movement allows for a more efficient random search of a target, which is well known and documented in the literature (Viswanathan et al., 1999; Bartumeus et al., 2005). However, this may not be true in general, as searching success could depend on the shape of the target boundary (see Fig. 4.2.4). This is not uncommon, as Brownian search strategies are known to become more advantageous under some conditions (e.g. presence of global bias), where it is shown that Lévy searchers can easily overshoot the target (Palyulin and Metzler., 2014).

On a final note, we would like to mention some limitations to this study which can possibly motivate further research work:

1. This study is limited to trap shapes which have been used in the field, namely, circular, square and slot, but, it would be interesting to consider other shapes, which are also used on occasion e.g. cross shaped traps (Perner and Schuler, 2004; Blackshaw et al., 2018).

2. Baars (1979) recorded that circular traps are slightly more efficient than square type, but this result could not be reproduced in a multi-trap setting with traps of the same shape. It is unclear whether our results on trap efficiency hold in such a scenario. This opens up additional questions related to how trapping efficiencies may alter with respect to various spatial arrangements. Our study provides a better understanding at the single trap level and thus a conceptual basis for investigating more complex settings, such as multi-trapping systems.

3. Our results are relevant to pitfall trapping studies with use of conventional traps. However, traps can be tailored to meet experimental requirements, and various designs have been developed to influence capture rates, e.g. baited traps (Rieske and Raffa, 1993), time-sorting traps (Chapman and Armstrong, 1997), barrier trapping (Desender and Maelfait, 1986), drift fences (Melbourne, 1999), ramps (Bostanian et al., 1983). Although applications are context specific and they are not as widely used, these alternatives still exist. For a better understanding of trap efficiencies in these cases, the modelling framework would need to be refined to account for the response due to these specific trap functions.

4. This study is primarily based on individual based modelling, but it is well known that the mean-field dynamics for BM, is well described by the diffusion equation (Petrovskii et al., 2012; Bearup et al.,

2015, 2016). It would be interesting to see a complimentary study that can reproduce our results in §4.1 at this level. In addition, trap counts could be further explored by considering more complicated movement types, which incorporate composite and/or intermittent behaviour, time/density dependent movement, interactions with the environment, etc. (Nathan et al., 2008; Codling, 2014).

5. Shlesinger and Klafter (1986) first introduced the concept of a LW in the biological literature with the proposal that such movement mechanisms could be observed in the foraging behaviour of ants. To the best of our knowledge, the extensive ecological literature does not contain empirical evidence that ground-dwelling arthropods perform LWs, even for a single species. Admittedly, any practical implications derived from our theoretical results on insects may be limited, but can be useful, more generally for animal movement.

6. From a more practical viewpoint, 'small' differences in trap efficiencies are not so much of a serious problem for field entomologists. There are other aspects linked to pitfall trapping still poorly understood, that need to be solved by both theoretical and field ecologists, e.g. why trap counts of ground-dwelling arthropods assemblages can provide a different record compared to techniques measuring population densities? Why some ground-dwelling arthropods are completely missing in pitfall trap samples and others are overestimated i.e. have low population densities but relatively high catches?

Acknowledgements

The authors are thankful to Aaron Ellison and three anonymous reviewers for their insightful comments. DA gratefully acknowledges the support given by Gulf University of Science and Technology (GUST), which was essential for the completion of this work. The publication has been prepared with the support of the "RUDN University Program 5-100" (to SP).

Author Contributions

DA and SP conceived the ideas. DA designed the methodology, ran the simulations and wrote the paper. SP revised the paper which substantially improved the manuscript.

Data Accessibility

The manuscript does not include any data.

Supplementary information

S1 Homogeneously distributed insects over the arena

In our simulations we assume that insects are homogeneously distributed over the arena at time $t = 0$. In mathematical terms, each initial position can be described as a random vector, written in polar co-ordinates $\mathbf{r}_0 = (r_0, \vartheta)$, where r_0 is the distance from the centre of the field, and ϑ is the angle subtended from the horizontal. The probability distribution can easily be written in the case of a circular arena with circular trap installed at the centre (3.1.1),

$$\lambda_0(r_0) = \frac{2r_0}{R_2^2 - R_1^2},\ R_1 < r_0 < R_2, \quad \psi_0(\vartheta) = \frac{1}{2\pi},\ -\pi < \vartheta \leq \pi, \tag{S1.1}$$

where the subscript in λ_0 and ψ_0 refers to 'initial'. For simulations, each individual position can be independently and randomly generated by

$$\mathbf{r}_0 \sim \left(\sqrt{\left(R_2^2 - R_1^2\right) U + R_1^2}, 2\pi U \right) \tag{S1.2}$$

where U is the uniform distribution defined over the interval from 0 to 1. This corresponds to uniformly distributed individuals over an annulus. In more complex geometries (asymmetrical under rotation) such as the square or slot trap cases, the probability distribution cannot be expressed analytically. Therefore, we devise the following methodology: a population of N_f individuals are uniformly distributed around the whole circular field $\mathbf{r}_0 \sim \left(R_2\sqrt{U}, 2\pi U\right)$, prior to the installation of the trap. Those individuals which happen to be situated within the trapping region are removed. As a result, the remaining population is uniformly distributed about the arena, with population, say $N_\omega < N_f$, where $\omega = 1$ corresponds to the square trap, and $\omega > 1$ for the slot trap. On assuming a constant population density ρ (number of insects per unit area), it follows that

$$\rho = \frac{N_f}{A_f} = \frac{N_\omega}{A_\omega} \ \Rightarrow\ \rho = \frac{N_f}{\pi R_2^2} = \frac{N_\omega}{\pi R_2^2 - \omega E^2}, \tag{S1.3}$$

where A denotes total area. From this we can determine an estimate for N_ω,

$$N_\omega = N_f \left(1 - \frac{\omega}{\pi} \left(\frac{E}{R_2} \right)^2 \right) \tag{S1.4}$$

which expresses the remaining population N_ω in terms of the population distributed around the whole field N_f, in the absence of a trap.

S2 Condition of equivalence: Correlated random walk vs Brownian motion

Consider the random walk framework as described in §2. The total displacement after n steps is given by,

$$\mathbf{R}_n = \sum_{i=0}^{n-1} (\mathbf{r}_{i+1} - \mathbf{r}_i) = \sum_{i=0}^{n-1} (\Delta \mathbf{r})_i \tag{S2.1}$$

where $(\Delta \mathbf{r})_i$ is the step vector as defined in (2.0.1). The corresponding mean squared displacement (MSD) derived by Kareiva and Shigesada (1983) reads,

$$E\left(R_n^2\right) = E\left(|\mathbf{R}_n|^2\right) = nE(l^2) + 2E(l)^2 \cdot \frac{(c-c^2-s^2)n - c}{(1-c)^2+s^2} + 2E(l)^2 \cdot \frac{2s^2 + (c^2+s^2)^{\frac{n+1}{2}}}{[(1-c)^2+s^2]^2} \cdot F(s,c) \tag{S2.2}$$

where

$$F(s,c) = \left((1-c)^2 - s^2\right)\cos\left((n+1)\arctan\left(\frac{s}{c}\right)\right) - 2s(1-c)\sin\left((n+1)\arctan\left(\frac{s}{c}\right)\right).$$

Here,

$$E(l) = \int_0^\infty l\lambda(l)dl, \quad E(l^2) = \int_0^\infty l^2\lambda(l)dl \tag{S2.3}$$

are the 1st and the 2nd moments of the step length distributions, respectively. For turning angles, such linear statistics cannot be used since any angular value is defined modulo 2π, so $\theta - \pi$ and $\theta + \pi$ correspond to the same direction (Codling et al., 2008). Useful moments for circular distributions include the mean sine s and mean cosine c, defined as

$$s = E(\sin\theta) = \int_{-\pi}^{\pi} \sin\theta\psi(\theta)d\theta, \quad c = E(\cos\theta) = \int_{-\pi}^{\pi} \cos\theta\psi(\theta)d\theta, \tag{S2.4}$$

and once these are computed for some given ψ, alongside (S2.3), then the MSD can be computed through (S2.2). Now consider the following cases:

Case 1 MSD for BM: Uniform turning angle $\psi(\theta) = \frac{1}{2\pi}$ with zero mean sines and cosines, $s = c = 0$. With this, (S2.2) reduces to

$$E(R_n^2) = nE(l^2) = n\int_0^\infty l^2\lambda(l;\sigma)dl = 2n\sigma^2. \tag{S2.5}$$

Case 2 MSD for the CRW: $\psi(\theta;\kappa)$ is the VMD given by (2.2.1) and due to symmetry we have that $s = 0$

and from (S2.2) we obtain

$$E(R_n^2) = nE(l^2) + 2E(l)^2 \frac{c}{1-c}\left(n - \frac{1-c^n}{1-c}\right). \tag{S2.6}$$

On computing moments, we have that

$$E(l) = \int_0^\infty l\lambda(l;\nu)dl = \frac{\nu\sqrt{2\pi}}{2}, \quad E(l^2) = \int_0^\infty l^2\lambda(l;\nu)dl = 2\nu^2, \quad c = \int_{-\pi}^{\pi} \cos\theta \cdot \frac{e^{\kappa\cos\theta}}{2\pi I_0(k)} d\theta = \frac{I_1(\kappa)}{I_0(\kappa)},$$

where $I_0(k)$ and $I_1(k)$ are defined through the integral $I_p(\kappa) = \frac{1}{2\pi}\int_{-\pi}^{\pi}\cos(p\theta)e^{\kappa\cos\theta}d\theta$, which denotes the p^{th} order modified Bessel function of the first kind. Substituting into (S2.6) we find that

$$E(R_n^2) = \nu^2\left\{2n + \pi \cdot \frac{\frac{I_1(\kappa)}{I_0(\kappa)}}{1-\frac{I_1(\kappa)}{I_0(\kappa)}}\left(n - \frac{1-\left(\frac{I_1(\kappa)}{I_0(\kappa)}\right)^n}{1-\left(\frac{I_1(\kappa)}{I_0(\kappa)}\right)}\right)\right\}. \tag{S2.7}$$

The condition of equivalence is obtained by equating the MSDs in (S2.5) and (S2.7), and on rearranging we have that

$$\nu = \sigma\left\{1 + \frac{\pi}{2} \cdot \frac{\frac{I_1(\kappa)}{I_0(\kappa)}}{1-\frac{I_1(\kappa)}{I_0(\kappa)}}\left(1 - \frac{1}{n} \cdot \frac{1-\left(\frac{I_1(\kappa)}{I_0(\kappa)}\right)^n}{1-\left(\frac{I_1(\kappa)}{I_0(\kappa)}\right)}\right)\right\}^{-\frac{1}{2}}. \tag{S2.8}$$

Finally, we can express the ratio of scale parameters in terms of concentration κ,

$$\frac{\nu}{\sigma} = \left\{1 + \frac{\pi}{2} \cdot \frac{\frac{I_1(\kappa)}{I_0(\kappa)}}{1-\frac{I_1(\kappa)}{I_0(\kappa)}}\left(1 - \frac{\Delta t}{t_i} \cdot \frac{1-\left(\frac{I_1(\kappa)}{I_0(\kappa)}\right)^{\frac{t_i}{\Delta t}}}{1-\left(\frac{I_1(\kappa)}{I_0(\kappa)}\right)}\right)\right\}^{-\frac{1}{2}}. \tag{S2.9}$$

with discretized time t_i instead of the number of steps n, see (2.0.1). In case of large time t_i and small but finite value of Δt, we have that $\frac{\Delta t}{t_i} \approx 0$, and therefore an approximation for (S2.9) reads,

$$\frac{\nu}{\sigma} \approx \left(1 + \frac{\pi}{2} \cdot \frac{\frac{I_1(\kappa)}{I_0(\kappa)}}{1-\frac{I_1(\kappa)}{I_0(\kappa)}}\right)^{-\frac{1}{2}} \tag{S2.10}$$

and in the infinite limit $t_i \to \infty$, $\frac{\Delta t}{t_i} \to 0$, (S2.9) reduces to

$$\frac{\nu}{\sigma} = \left(1 + \frac{\pi}{2} \cdot \frac{\frac{I_1(\kappa)}{I_0(\kappa)}}{1-\frac{I_1(\kappa)}{I_0(\kappa)}}\right)^{-\frac{1}{2}} \tag{S2.11}$$

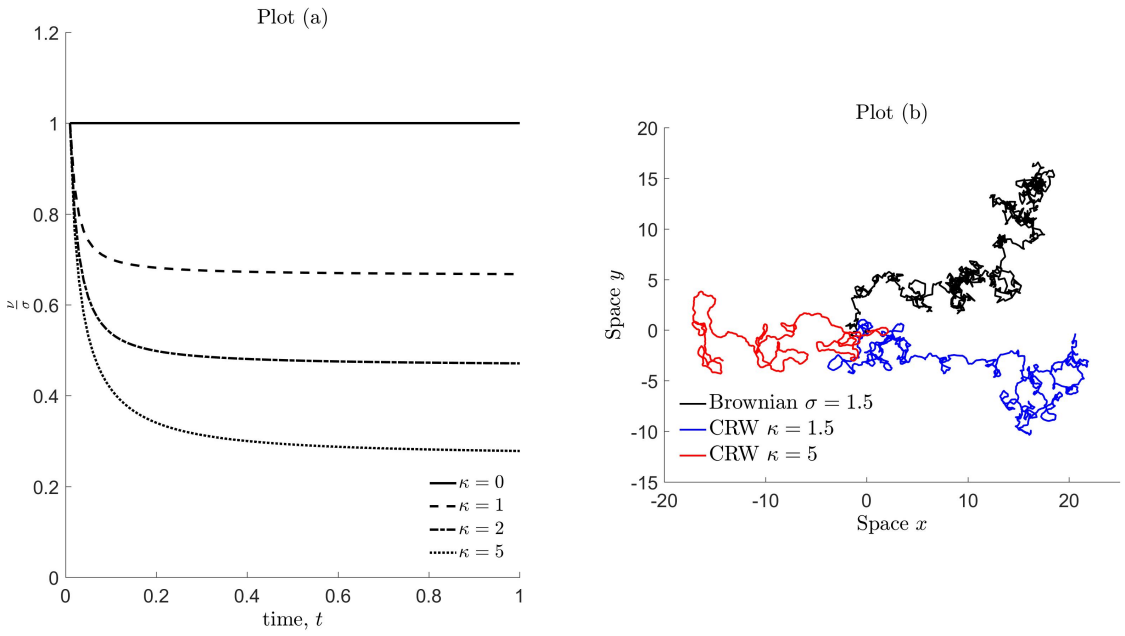

Figure S2.1: Plot (a) Condition of equivalence (S2.9) plotted against time t_i with $\Delta t = 0.01$, for varying concentrations $\kappa = 0, 1, 2, 5$. Plot (b) Sample random walks with $n = 1000$ steps for (i) BM $\sigma = 0.3$ (black), (ii) CRW with low forward persistence $\kappa = 1.5$ (blue) and (iii) CRW with high forward persistence $\kappa = 5$ (red). Note that, the CRW parameter v varies at each time step, and is determined from (S2.9).

which is constant for fixed κ. As a result, the ratio of scale parameters is time invariant for sufficiently large time, as observed in Fig. S2.1(a). Note that, in the special case $\kappa = 0$ (no forward persistence) the VMD in (2.2.1) is the uniform distribution $\psi(\theta; \kappa = 0) = \frac{1}{2\pi}$, and the CRW reduces to BM with equal scale parameters, $v = \sigma$, as expected. Fig. S2.1(b) illustrates typical sample paths for BM and the CRW with low/high forward persistence. Here, the scale parameters are related through the condition of equivalence (S2.9) which ensures that each trajectory has the exact same MSD. We observe completely random movement for BM, whereas, for the CRW the movement is more directed with less 'tangles' and 'turns'.

S3 Condition of equivalence: Lévy walk vs Brownian motion

As a technical note, the terminology '*Lévy flight*' or '*Lévy walk*' is synonymous in the biological literature. The subtle difference is that, Lévy flights allow for arbitrarily large steps, which can theoretically result in non-physical infinite velocities, whereas LWs ensure that the propagation velocity is finite. Note that, in the physical sciences more caution is taken and a clear distinction is made (Dybiec et al., 2017). To avoid any unnecessary confusion, throughout the study, we use Lévy walks as a reference to a random walk whose step distribution has the asymptotic property (2.3.1), although technically, this is a Lévy flight.

Lévy walks are scale-free in the sense that the variance of the step length distribution is divergent. The MSD is unbounded and grows ballistically or sub-ballistically over time (Klafter et al., 1987). The usual methodology used to relate scale-specific movement processes through equating the MSD (as outlined in §S2) cannot be applied. To overcome this, an alternative approach allows a characteristic scale length L to be defined, by fixing the probability ε of executing a step not exceeding L,

$$P(l < L) = \varepsilon \tag{S3.1}$$

also known as a survival or exceedance probability. In the literature on individual animal movement, there are some arguments that LWs are never really scale-free, since terminology can be misleading. A characteristic step length can 'always' be defined, but may be described somewhat differently, either through the median, geometric-averages, or even based on dimensional analysis (Kawai and Petrovskii, 2012). Although such approaches are plausible, they are hardly ever used and not favourable. A quick scope of recent literature will demonstrate that the usual methodology is through equating survival probabilities, e.g. Rodrigues et al. (2015); Bearup et al. (2016); Choules and Petrovskii (2017); Ellis et al. (2018) and there are many others. The motivation stems from the idea that step lengths can be divided into two classes, short range steps $l < L$ and long range steps $l > L$, with probabilities ε and $1-\varepsilon$, respectively.

To obtain a condition of equivalence between BM and the LW, firstly, we need an expression for L. From (S3.1) we can derive the following for Brownian step lengths,

$$\int_0^L \lambda(l;\sigma)dl = \int_0^L \frac{l}{\sigma^2}\exp\left(-\frac{l^2}{2\sigma^2}\right)dl = \varepsilon \;\Rightarrow\; L = \sqrt{-2\sigma^2\ln(1-\varepsilon)}, \tag{S3.2}$$

and for the Lévy step length distribution,

$$\int_0^L \lambda(l;\gamma)dl = \int_0^L \frac{2\gamma}{\pi(\gamma^2+l^2)}dl = \varepsilon \;\Rightarrow\; L = \gamma\tan\left(\frac{\pi\varepsilon}{2}\right). \tag{S3.3}$$

To enforce equivalence, we assume that this characteristic length is the same, and therefore we can eliminate L from (S3.2) - (S3.3) and rearrange to obtain

$$\zeta(\varepsilon) = \frac{\gamma}{\sigma} = \sqrt{-2\ln(1-\varepsilon)}\cot\left(\frac{\pi\varepsilon}{2}\right), \tag{S3.4}$$

which expresses the ratio of scale-parameters ζ purely in terms of probability ε. The basic idea is that for chosen ε, the value of ζ can be computed from (S3.4), and therefore a conditional relation of the form $\gamma = \zeta\sigma$ can be sought. The issue is that the value of ε is always chosen arbitrarily, without any clear reasoning. Some typical choices are $\varepsilon = 0.1, 0.5, 0.9$ (Rodrigues et al. (2015); Bearup et al. (2016); Choules and Petrovskii (2017); Ellis et al. (2018)). To overcome this issue, we introduce the following

optimization technique to uniquely determine the optimal probability ε^*.

Firstly, consider the $\mathscr{L}_2$ norm defined as,

$$\mathscr{L}_2(\gamma,\sigma)=\left(\int_0^\infty\left(\lambda(l;\gamma)-\lambda(l;\sigma)\right)^2 dl\right)^{\frac{1}{2}} \tag{S3.5}$$

which computes the squared distance between the step length distributions. For the LW (with Folded Cauchy distribution) and BM we have that,

$$\mathscr{L}_2(\gamma,\sigma)=\left(\int_0^\infty\left(\frac{2\gamma}{\pi(\gamma^2+l^2)}-\frac{l}{\sigma^2}\exp\left(-\frac{l^2}{2\sigma^2}\right)\right)^2 dl\right)^{\frac{1}{2}} \tag{S3.6}$$

which can be evaluated analytically,

$$\mathscr{L}_2(\gamma,\sigma)=\left(\frac{\sqrt{\pi}}{4\sigma}-\frac{2\gamma}{\pi\sigma^2}\exp\left(\frac{\gamma^2}{2\sigma^2}\right)\mathrm{E}_1\left(\frac{\gamma^2}{2\sigma^2}\right)+\frac{1}{\pi\gamma}\right)^{\frac{1}{2}} \tag{S3.7}$$

where $\mathrm{E}_1(z)=\int_z^\infty\frac{e^{-t}}{t}dt$ is a form of the exponential integral (Abramowitz and Stegun, 1972). On substituting $\zeta=\frac{\gamma}{\sigma}$, the above can be written as

$$\mathscr{L}_2(\varepsilon;\sigma)=\frac{1}{\sqrt{\pi\sigma}}\cdot\left(\frac{\pi\sqrt{\pi}}{4}-2\zeta\exp\left(\frac{\zeta^2}{2}\right)\mathrm{E}_1\left(\frac{\zeta^2}{2}\right)+\frac{1}{\zeta}\right)^{\frac{1}{2}} \tag{S3.8}$$

with $\zeta=\zeta(\varepsilon)$ given by (S3.4). We now seek to solve the following optimization problem, that is, to determine the value of $\varepsilon=\varepsilon^*$ which minimizes the norm (S3.8).

The derivative of (S3.8) reads,

$$\frac{d\mathscr{L}_2}{d\varepsilon}=\frac{d\mathscr{L}_2}{d\zeta}\cdot\frac{d\zeta}{d\varepsilon}=-\frac{G(\varepsilon)}{2\pi\sigma\mathscr{L}_2}\cdot\frac{d\zeta}{d\varepsilon} \tag{S3.9}$$

where

$$G(\varepsilon)=\frac{1}{\zeta^2}-2\left(1+\zeta^2\right)\exp\left(\frac{\zeta^2}{2}\right)\mathrm{E}_1\left(\frac{\zeta^2}{2}\right)-4 \tag{S3.10}$$

is the optimality function. It follows that the optimal probability is a solution of the equation $G(\varepsilon^*)=0$ which can easily be computed numerically.

Fig. S3.1 (a) - (c) shows that the $\mathscr{L}_2$ norm is minimized at $\varepsilon^*=0.342$ (to 3.d.p), and is invariant with respect to σ. Plot (d) shows the optimality function $G(\varepsilon)$, and this optimal probability is a zero of this function. Plot (e) demonstrates equivalent step length distributions in the case of BM with $\sigma=0.5,1,3$ and the LW with $\gamma=0.768,1.536,4.608$, respectively. The condition of equivalence between these scale

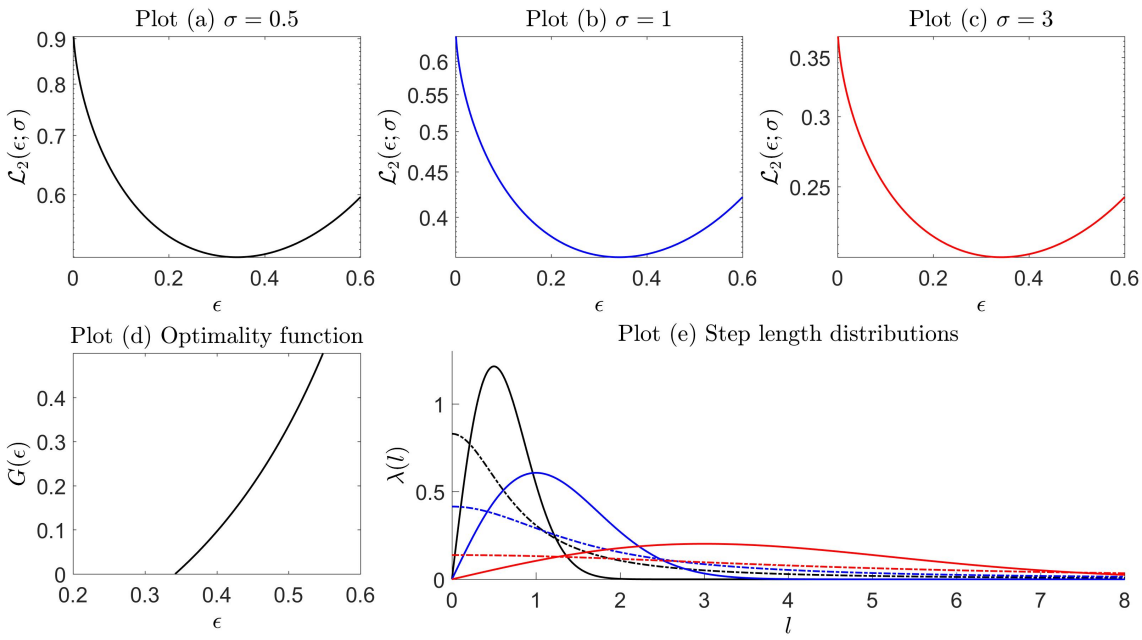

Figure S3.1: Semi-log plots of the $\mathscr{L}_2$ norm given by (S3.8) for different values of (a) $\sigma = 0.5$ (black), (b) $\sigma = 1$ (blue) and (c) $\sigma = 3$ (red). (d) Optimality function $G(\varepsilon)$ given by (S3.10). (e) Equivalence obtained between step length distributions, namely, the Weibull distribution (2.1.1) with $\sigma = 0.5$ (black solid), $\sigma = 1$ (blue solid) $\sigma = 3$ (red solid) and Folded-Cauchy distribution (2.3.2) with $\gamma = 0.768$ (black dashed), $\gamma = 1.536$ (blue dashed), $\gamma = 4.608$ (red dashed). Corresponding parameters are determined from $\gamma = \zeta^*\sigma$ with $\zeta^* = 1.536$ and optimal probability $\varepsilon^* = 0.342$.

parameters is given by,

$$\gamma = \zeta^*\sigma \quad \text{with} \quad \zeta^* = 1.536 \tag{S3.11}$$

which ensures that for both movement processes, the probability of executing the same step size of at most length L is fixed at $\varepsilon^* = 0.342$, subject to the 'similarity' constraint that the squared distance between the step length distributions is minimized. The advantage of this methodology is that ε^* is optimal and now unique, rather than chosen arbitrarily. Of course, other constraints are possible such as minimizing the $\mathscr{L}_1$ norm, which is equivalent to minimizing the area between the distributions, however, in this case the norm is not analytically tractable, and also cannot be generalized since ε^* varies with σ. The methodology outlined in this section can be easily extended to compare random walks for a variety of step length distributions where at least one of them has a divergent variance. An upcoming paper aims to deal with this issue in more detail (Ahmed and Bearup, 2019).

References

Abramowitz, M. and Stegun, I. (1972). *Handbook of mathematical functions*. Washington: National Bureau of Standards.

Ahmed, D. (2015). *Stochastic and Mean field approaches for trap counts modelling and interpretation*. PhD thesis, University of Leicester, UK.

Ahmed, D. and Bearup, D. (2019). Establishing equivalence between Brownian Motion and Lévy Flights. In prep.

Ahmed, D. and Petrovskii, S. (2015). Time Dependent Diffusion as a Mean Field Counterpart of Lévy Type Random Walk. *Math. Model. Nat. Phenom.*, 10(2):5 – 26.

Ahmed, D., Petrovskii, S., and Tilles, P. (2018). The Lévy or Diffusion Controversy: How Important Is the Movement Pattern in the Context of Trapping? *Mathematics*, 6(77). https://doi.org/10.3390/math6050077.

Allema, A., van der Werf, W., Groot, J., Hemerik, L., Gort, G., Rossing, W., and van Lenteren, J. (2015). Quantification of motility of carabid beetles in farmland. *Bull. Entomol. Res.*, 105(2):234 – 44.

Auger-Méthé, M., Derocher, A., Plank, M., and Codling, E. (2015). Differentiating the Lévy walk from a composite correlated random walk. *Methods Ecol. Evol.*, 6(10):1179 – 1189.

Baars, M. (1979). Catches in pitfall traps in relation to mean densities of carabid beetles. *Oecologia*, 41(1):25 – 46.

Bailey, J., Wallis, J., and Codling, E. (2018). Navigational efficiency in a biased and correlated random walk model of individual animal movement. *Ecology*, 99(1):217 – 223.

Bartumeus, F. and Catalan, J. (2009). Optimal search behavior and classic foraging theory. *J. Phys. A: Math. Theor.*, 42(43):569 – 580.

Bartumeus, F., Da Luz, M., Viswanathan, G., and Catalan, J. (2005). Animal search strategies: A quantitative random-walk analysis. *Ecology*, 86(11):3078 – 87.

Bearup, D., Benefer, C., Petrovskii, S., and Blackshaw, R. (2016). Revisiting Brownian motion as a description of animal movement: a comparison to experimental movement data. *Methods Ecol. Evol.*, 7(12):1525 – 37.

Bearup, D., Petrovskaya, N., and Petrovskii, S. (2015). Some analytical and numerical approaches to understanding trap counts resulting from pest insect immigration. *Math. Biosci.*, 263:143 – 160.

Bearup, D. and Petrovskii, S. (2015). On time scale invariance of random walks in confined space. *J. Theor. Biol.*, 367:230 – 245.

Berec, L., Kean, J., Epanchin-Niell, R., Liebhold, A., and Haight, R. (2015). Designing efficient surveys: spatial arrangement of sample points for detection of invasive species. *Biological Invasions*, 17(1):445 – 459.

Berg, H. (1983). *Random Walks in Biology.* Princeton University Press.

Bergman, C., Schaefer, J., and Luttich, S. (2000). Caribou movement as a correlated random walk. *Oecologia*, 123(3):364 – 374.

Blackshaw, R., Vernon, R., and Thiebaud, F. (2018). Large scale Agriotes spp. click beetle (Coleoptera: Elateridae) invasion of crop land from field margin reservoirs. *Agric. For. Entomol.*, 20(1):51 – 61.

Boetzl, F., Ries, E., Schneider, G., and Krauss, J. (2018). Its a matter of design - how pitfall trap design affects trap samples and possible predictions. *Peer. J.*, 6:e5078. https://doi.org/10.7717/peerj.5078.

Bostanian, N., Boivin, G., and Goulet, H. (1983). Ramp Pitfall Trap. *J. Econ. Entomol.*, 76(6):1473 – 75.

Bovet, P. and Benhamou, S. (1988). Spatial analysis of animals' movements using a correlated random walk model. *J. Theor. Biol.*, 131(4):419 – 433.

Brown, G. and Matthews, I. (2016). A review of extensive variation in the design of pitfall traps and a proposal for a standard pitfall trap design for monitoring ground-active arthropod biodiversity. *Ecol. Evol.*, 6(12):3953 – 64.

Byers, J. (2001). Correlated random walk equations of animal dispersal resolved by simulation. *Ecology*, 82(6):1680 – 90.

Carslaw, H. and Jaeger, J. (1959). *Conduction of heat in solids*. Clarendon Press, Oxford, 1st edition.

Chapman, P. and Armstrong, G. (1997). Design and use of a time-sorting pitfall trap for predatory arthropods. *Agr. Ecosyst. Environ.*, 65(1):15 – 21.

Cheli, G. and Corley, J. (2010). Efficient sampling of ground-dwelling arthropods using pitfall traps in arid steppes. *Neotrop. Entomol.*, 39(6):912 – 917.

Choules, J. and Petrovskii, S. (2017). Which Random Walk is Faster? Methods to Compare Different Step Length Distributions in Individual Animal Movement. *Math. Model. Nat. Phenom.*, 12(2):22 – 45.

Codling, E. (2014). Pest insect movement and dispersal as an example of applied movement ecology. Comment on "Multiscale approach to pest insect monitoring: random walks, pattern formation, synchronization, and networks" by Petrovskii, Petrovskaya and Bearup. *Phys. Life Rev.*, 11(3):533 – 535.

Codling, E. and Plank, M. (2011). Turn designation, sampling rate and the misidentification of power laws in movement path data using maximum likelihood estimates. *Theor. Ecol. 4.3 (2011): 397-406.*, 4(3):397 – 406.

Codling, E., Plank, M., and Benhamou, S. (2008). Random walk models in biology. *J. R. Soc. Interface*, 5(25):813 – 834.

Császár, P., Torma, A., Gallé-Szpisjak, N., Tölgyesi, C., and Gallé, R. (2018). Efficiency of pitfall traps with funnels and/or roofs in capturing ground-dwelling arthropods. *Eur. J. Entomol.*, 115:15 – 24.

De Jager, M., Weissing, F., Herman, P., Nolet, B., and van de Koppel, J. (2012). Response to Comment on "Lévy Walks Evolve Through Interaction Between Movement and Environmental Complexity". *Science*, 335(6071):918.

Den Boer, P. (1981). On the survival of populations in a heterogeneous and variable environment. *Oecologia*, 50:39 – 53.

Desender, K. and Maelfait, J. (1986). Pitfall trapping with enclosures: a method for estimating the relationship between the abundances of coexisting carabid species (Coleoptera: Carabidae). *Holarctic Ecol.*, 9:245 – 250.

Dybiec, B., Gudowska-Nowak, E., Barkai, E., and Dubkov, A. (2017). Lévy flights versus Lévy walks in bounded domains. *Phys. Rev. E.* doi: 10.1103/PhysRevE.95.052102.

Edwards, A., Phillips, R., Watkins, N., Freeman, M., Murphy, E., Afanasyev, V., et al. (2007). Revisiting Lévy flight search patterns of wandering albatrosses, bumblebees and deer. *Nature*, 449(7165):1044 – 1048.

Edwards, A. M. (2011). Overturning conclusions of lévy flight movement patterns by fishing boats and foraging animals. *Ecology*, 926:1247 – 57.

El-Sayed, A., Suckling, D., Wearing, C., and Byers, J. (2006). Potential of mass trapping for long term pest management and eradication of invasive species. *Journal of Economic Entomology*, 99:1550 – 1564.

Ellis, J., Petrovskaya, N., and Petrovskii, S. (2018). Effect of density-dependent individual movement on emerging spatial population distribution: Brownian motion vs Lévy flights. *J. Theor. Bio.*, 464:159 – 178.

Engel, J., Hertzog, L., Tiede, J., Wagg, C., Ebeling, A., Briesen, H., and Weisser, W. (2017). Pitfall trap sampling bias depends on body mass, temperature, and trap number: insights from an individual-based model. *Ecosphere*, 8(4).

Fagan, W. and Calabrese, J. (2014). The Correlated Random Walk and the Rise of Movement Ecology. *Bull. Ecol. Soc. Am.*, 95(3):204 – 206.

Fisher, N. (1995). *Statistical Analysis of Circular Data*. Cambridge University Press.

Focardi, S., Montanaro, P., and Pecchioli, E. (2009). Adaptive Lévy Walks in Foraging Fallow Deer. *PLoS One*, 4(8). https://doi.org/10.1371/journal.pone.000658.

Giblin-Davis, R., Peña, J., and Duncan, R. (1994). Lethal pitfall trap for the evaluation of semiochemical-mediated attraction of metamasius hemipterus sericeus (coleoptera: Curculionidae). *Florida Entomologist*, 77:247 – 255.

Greenslade, P. (1964). Pitfall Trapping as a Method for Studying Populations of Carabidae (Coleoptera). *J. Animal Ecol.*, 33(2):301 – 310.

Grevstad, F. and Herzig, A. (1997). Quantifying the effects of distance and conspecifics on colonization: experiments and models using the loosestrife leaf beetle, galerucella calmariensis. *Oecologia*, 110:60 – 68.

Grimm, V. and Railsback, S. (2005). *Individual-based Modeling and Ecology.* Princeton University Press.

Halsall, N. and Wratten, S. (1988). The efficiency of pitfall trapping for polyphagous predatory Carabidae. *Ecol. Ent.*, 13:293 – 299.

Hammond, P. (1990). *Insect abundance and diversity in the Dumoga-Bone national park, N.Sulawesi, with special reference to the beetle fauna of lowland rain forest in the Toraut region.* The Royal Entomological Society of London, London, in insects and rainforests of south east asia (wallacea) (ed. w.j. knight j.d. holloway) edition. pp. 197 – 254.

Hannunen, S. (2005). Modelling the interplay between pest movement and the physical design of trap crop systems. *Agric For Entomol*, 7(1):11 – 20.

Hapca, S., Crawford, J., and Young, I. (2009). Anomalous diffusion of heterogeneous populations characterized by normal diffusion at the individual level. *Journal of the Royal Society Interface*, 6:111 – 122.

Hengeveld, R. (1989). *Dynamics of Biological Invasions*. Chapman and Hall: London, UK.

Holden, M., Ellner, S., Lee, D., Nyrop, J., and Sanderson, J. (2012). Designing an effective trap cropping strategy: the effects of attraction, retention and plant spatial distribution. *Journal of Applied Ecology*, 49(3):715 – 722.

Holmes, E. (1993). Are diffusion models too simple? a comparison with telegraph models of invasion. *Am. Nat.*, 142(5):779 – 795.

Honêk, A. (1988). The effect of crop density and microclimate on pitfall trap catches of carabidae, staphylinidae (coleoptera) and lycosidae (araneae) in cereal fields. *Pedobiologia*, 32(233 – 242).

Humphries, N., Queiroz, N., Dyer, J., Pade, N., Musyl, M., Schaefer, K., et al. (2010). Environmental context explains Lévy and Brownian movement patterns of marine predators. *Nature*, 465(7301):1066 – 9.

Iwao, S. and Machida, A. (1963). A marking-and-recapture analysis of the adult population of a phytophagous lady-beetle, epilachna sparsa orientalis. *Researched on Population Ecology*, 5(2):107 – 116.

Kareiva, P. and Shigesada, N. (1983). Analyzing insect movement as a correlated random walk. *Oecologia*, 56(2 – 3):234 – 238.

Kawai, R. and Petrovskii, S. (2012). Multiscale properties of random walk models of animal movement: lessons from statistical inference. *Proc R Soc*, 468:1428 – 1451.

Klafter, J., Blumen, A., and Shlesinger, M. (1987). Stochastic pathway to anomalous diffusion. *Phys Rev A Gen Phys*, 35(7):3081 – 3085.

Knell, A. and Codling, E. (2012). Classifying area-restricted search (ARS) using a partial sum approach. *Theor. Ecol.*, 5(3):325 – 329.

Koivula, M., Kotze, D., Hiisivuori, L., and Rita, H. (2003). Pitfall trap efficiency: do trap size, collecting fluid and vegetation structure matter? *Entomol. Fennica.*, 14:1 – 14.

Levin, S., Cohen, D., and Hastings, A. (1984). Dispersal strategies in patchy environments. *Theor. Popul. Biol.*, 26:165 – 180.

Luff, M. (1975). Some features influencing the efficiency of pitfall traps. *Oecologia*, 19(4):345 – 357.

Mashanova, A., Olive, T., and Jansen, V. (2010). Evidence for intermittency and a truncated power law from highly resolved aphid movement data. *J. R. Soc. Interface*, 7:199 – 208.

Masó, J. (2015). *Factors influencing the mobility of Red palm weevil Rhynchophorus ferrugineus (Coleoptera: Dryophthoridae) adults*. PhD thesis, Universitat Politécnica de Valéncia, Institute of Mediterranean Agroforestry (IAM).

McEvoy, P. B. (1977). *Adaptive significance of clumped dispersion in treehopper, Publilia concava (Homoptera: Membracidae)*. Dissertation thesis, Cornell University.

Melbourne, B. (1999). Bias in the effect of habitat structure on pitfall traps: An experimental evaluation. *Aust. J. Ecol.*, 24(3):228 – 239.

Miller, J., Adams, C., Weston, P., and Schenker, J. (2015). *Trapping of Small Organisms Moving Randomly. Principles and Applications to Pest Monitoring and Management.* United States: Springer. Springer briefs in ecology.

Mommertz, S., Schauer, C., Kösters, N., Lang, A., and Filser, J. (1996). A comparison of d-vac suction, fenced and unfenced pitfall trap sampling of epigeal arthropods in agroecosystems. *Annales Zoolgica Fennici*, 33:117 – 124.

Morales, J., Haydon, D., Frair, J., Holsinger, K., and Fryxell, J. (2004). Extracting more out of relocation data: building movement models as mixtures of random walks. *Ecology*, 85(9):2436 – 45.

Nathan, R., Getz, W., Revilla, E., Holyoak, M. Kadmon, R., and Saltz, D. (2008). A movement ecology paradigm for unifying organismal movement research. *Proc Natl Acad Sci USA*, 105:19052 – 9.

Niemelä, J., Halme, E., and Haila, Y. (1990). Balancing sampling effort in pitfall trapping of carabid beetles. *Entomologica Fennica*, 1:233 – 238.

Okubo, A. (1980). *Diffusion and Ecological Problems: Mathematical Models.* Springer, Berlin.

Palyulin, V.V., A. V. C. and Metzler., R. (2014). Lévy flights do not always optimize random blind search for sparse targets. *Proc Natl Acad Sci USA*, 111(8):2931 – 36.

Pearce, J., Schuurman, D., Barber, K., Larrivée, M., Venier, L., McKee, J., and McKenney, D. (2005). Pitfall trap designs to maximize invertebrate captures and minimize captures of nontarget vertebrates. *Can. entomol.*, 137(2):233 – 250.

Pekár, S. (2002). Differential effects of formaldehyde concentration and detergent on the catching efficiency of surface active arthropods by pitfall traps. *Pedobiologia*, 46(6):539 – 547.

Perner, J. and Schuler, S. (2004). Estimating the density of ground-dwelling arthropods with pitfall traps using a nested-cross array. *J. Anim. Ecol*, 73(3):469 – 447.

Petrovskii, S., Bearup, D., Ahmed, D., and Blackshaw, R. (2012). Estimating insect population density from trap counts. *Ecol. complexity*, 10:69 – 82.

Petrovskii, S., Mashanova, A., and Jansen, V. (2011). Variation in individual walking behavior creates the impression of a Lévy flight. *Proc. Natl. Acad. Sci. USA*, 108(21):8704 – 07.

Petrovskii, S. and Morozov, A. (2009). Dispersal in a statistically structured population: fat tails revisited. *Am. Nat.*, 173(2):278 – 289.

Petrovskii, S. and Petrovskaya, N. (2012). Computational ecology as an emerging science. *Interface Focus*, 2(2):241 – 254.

Petrovskii, S., Petrovskya, N., and Bearup, D. (2014). Multiscale approach to pest insect monitoring: random walks, pattern formation, synchronization and networks. *Phys. Life Rev.*, 11(3):467 – 525.

Pimentel, D. (2009). *Integrated pest management: innovation-development process.*, volume 1. Berlin: Springer. pages: 83 – 88.

Plank, M. and Codling, E. (2009). Sampling rate and misidentification of l and non-l movement paths. *Ecology*, 90:3546 – 3553.

Pyke, G. (2015). Understanding movements of organisms: It's time to abandon the Lévy foraging hypothesis. *Methods Ecol. Evol.*, 6(1):1 – 16.

Reichenbach, T., Mobilia, M., and Frey, E. (2007). Mobility promotes and jeopardizes biodiversity in rock-paper-scissors games. *Nature*, 448:1046 – 1049.

Reynolds, A. (2012). Olfactory search behaviour in the wandering albatross is predicted to give rise to Lévy flight movement patterns. *Anim. Behav.*, 83:1225 – 29.

Reynolds, A. (2018). Current status and future directions of Lévy walk research. *Biology Open*. Published by The Company of Biologists Ltd.

Rieske, L. and Raffa, K. (1993). Potential Use of Baited Pitfall Traps in Monitoring Pine Root Weevil, Hylobius pales, Pachylobius picivorus, and Hylobius radicis (Coleoptera: Curculionidae) Populations and Infestation Levels. *J. Econ. Entomol.*, 86(2):475 – 485.

Rodrigues, L., Mistro, D., Cara, E., Petrovskaya, N., and Petrovskii, S. (2015). Patchy Invasion of Stage-Structured Alien Species with Short-Distance and Long-Distance Dispersal. *Bull. Math. Biol.*, 77(8):1583 – 619.

Saska, P., van der Werf, W., Hemerik, L., and Luff, M. (2013). Temperature effects on pitfall catches of epigeal arthropods: a model and method for bias correction. *J. Appl. Ecol.*, 50:181 – 189.

Sendova, A. and Lent, J. (2012). Random walk models of worker sorting in ant colonies. *J Theor Bio*, 217(2):255 – 274.

Shlesinger, M. and Klafter, J. (1986). *Lévy walks versus Lévy flights*. Martinus Nijhof Publishers, Amsterdam, in: stanley, h.e., ostrowski, n. (eds.), growth and form edition. pp. 279 – 283.

Sims, D., Southall, E., Humphries, N., Hays, G., Bradshaw, C., Pitchford, J., James, A., Ahmed, M., Brierley, A., Hindell, M., Morritt, D., Musyl, M., Righton, D., Shepard, E., Wearmouth, V., Wilson, R., Witt, M., and Metcalfe, J. (2008). Scaling laws of marine predator search behaviour. *Nature*, 451:1098 – 102.

Sornette, D. (2004). *Critical Phenomena in Natural Sciences*. Berlin, Springer, 2nd edition.

Southwood, T. (1978). *Ecological Methods*. Chapman and Hall, London, 2nd edition.

Spence, J. and Niemelä, J. (1994). Sampling carabid assemblages with pitfall traps: The madness and the method. *Can. Entomol.*, 126(3):881 – 894.

Strauss, W. (2008). *Partial differential equations: An introduction*. John Wiley Sons., 2nd edition.

Turchin, P. (1998). *Quantitative analysis of movement. Measuring and modelling population redistribution in animals and plants.* Sinauer Associates, Inc. Sunderland, Massachusetts.

Viswanathan, G., Buldyrev, S., Havlin, S., Luz, M., Raposo, E., and Stanley, H. (1999). Optimizing the success of random searches. *Nature*, 401:911 – 914.

968 Watanabe, M. (1978). Adult movements and resident ratios of the black-veined white, aporia crataeyi, in
969 a hilly region. *Jap J Ecol*, 28:101 – 109.

970 Weiss, G. H. (1994). *Aspects and applications of the random walk*. Amsterdam, The Netherlands: North
971 Holland Press.

972 Woodcock, B. (2005). *Insect sampling in forest ecosystems*. Blackwell Science ltd. Chapter 3.

973 Work, T., Buddle, C., Korinus, L., and Spence, J. (2002). Pitfall trap size and capture of three taxa of
974 litterdwelling arthropods: implications for biodiversity studies. *Environ. Entomol.*, 31:438 – 448.